3. Tsuchiya-Suzuki A, Yazaki M, Nakamura A, et al. Clinical and genetic features of familial Mediterranean fever in Japan. *J Rheumatol*. 2009; 36(8):1671–1676.
4. Iwata K, Toma T, Yachie A, et al. Case of recurrent fever with apparent response to antibiotic: Overcoming "CRP dependency". *General Medicine*. 2011;12(1):29–31.
5. Yamane T, Uchiyama K, Hata D, et al. A Japanese case of familial Mediterranean fever with onset in the fifties. *Intern Med*. 2006;45(8): 515–517.
6. Tunca M, Akar S, Onen F, et al. Familial Mediterranean fever (FMF) in Turkey: results of a nationwide multicenter study. *Medicine (Baltimore)*. 2005;84(1):1–11.
7. Pras E, Livneh A, Balow JE Jr, et al. Clinical differences between North African and Iraqi Jews with familial Mediterranean fever. *Am J Med Genet*. 1998;75(2):216–219.
8. Saito M, Nishikomori R, Kambe N. Familial Mediterranean fever: MEFV gene mutations and treatment. *Nihon Rinsho Meneki Gakkai Kaishi*. 2007;30(2):78–85. Japanese.
9. Migita K, Nakamura T, Maeda Y, et al. MEFV mutations in Japanese rheumatoid arthritis patients. *Clin Exp Rheumatol*. 2008;26(6): 1091–1094.
10. Ryan JG, Masters SL, Booty MG, et al. Clinical features and functional significance of the P369S/R408Q variant in pyrin, the familial Mediterranean fever protein. *Ann Rheum Dis*. 2010;69(7):1383–1388.
11. Shimizu M, Tone Y, Toga A, et al. Colchicine-responsive chronic recurrent multifocal osteomyelitis with MEFV mutations: a variant of familial Mediterranean fever? *Rheumatology (Oxford)*. 2010;49(11): 2221–2223.
12. Ayaz NA, Ozen S, Bilginer Y, et al. MEFV mutations in systemic onset juvenile idiopathic arthritis. *Rheumatology (Oxford)*. 2009;48(1): 23–25.
13. Touitou I, Magne X, Molinari N, et al. MEFV mutations in Behçet's disease. *Hum Mutat*. 2000;16(3):271–272.
14. Ben-Chetrit E, Cohen R, Chajek-Shaul T. Familial mediterranean fever and Behçet's disease – are they associated? *J Rheumatol*. 2002;29(3): 530–534.
15. Atagunduz P, Ergun T, Direskeneli H. MEFV mutations are increased in Behçet's disease (BD) and are associated with vascular involvement. *Clin Exp Rheumatol*. 2003;21(4 Suppl 30):S35–S37.
16. Imirzalioglu N, Dursun A, Tastan B, Soysal Y, Yakicier MC. MEFV gene is a probable susceptibility gene for Behçet's disease. *Scand J Rheumatol*. 2005;34(1):56–58.
17. Ozen S, Bakkaloglu A, Yilmaz E, et al. Mutations in the gene for familial Mediterranean fever: do they predispose to inflammation? *J Rheumatol*. 2003;30(9):2014–2018.

Int J Hematol (2012) 96:443–449
DOI 10.1007/s12185-012-1156-0

ORIGINAL ARTICLE

Clonal expansion of Epstein–Barr virus (EBV)-infected γδ T cells in patients with chronic active EBV disease and hydroa vacciniforme-like eruptions

Taizo Wada · Akiko Toga · Yasuhisa Sakakibara · Tomoko Toma · Minoru Hasegawa · Kazuhiko Takehara · Tomonari Shigemura · Kazunaga Agematsu · Akihiro Yachie

Received: 26 May 2012 / Revised: 27 July 2012 / Accepted: 30 July 2012 / Published online: 12 August 2012

Abstract Chronic active Epstein–Barr virus (EBV) disease (CAEBV) is a systemic EBV-positive lymphoproliferative disorder characterized by fever, lymphadenopathy, and splenomegaly. Patients with CAEBV may present with cutaneous symptoms, including hypersensitivity to mosquito bites and hydroa vacciniforme (HV)-like eruptions. HV is a rare photodermatosis characterized by vesicles and crust formation after exposure to sunlight, with onset in childhood, and is associated with latent EBV infection. While γδ T cells have recently been demonstrated to be the major EBV-infected cell population in HV, the immunophenotypic features of EBV-infected γδ T cells in CAEBV with HV-like eruptions or HV remain largely undetermined. We describe three patients with CAEBV whose γδ T cells were found to be the major cellular target of EBV. HV-like eruptions were observed in two of these patients. A clonally expanded subpopulation of γδ T cells that were highly activated and T cell receptor Vγ9- and Vδ2-positive cells was demonstrated in all patients. We also show that the clonally expanded γδ T cells infiltrated into the HV-like eruptions in one patient from whom skin biopsy specimens were available. These results suggest the pathogenic roles of clonally expanded γδ T cells infected by EBV in patients with CAEBV and HV-like eruptions.

Keywords Epstein–Barr virus · Clonal proliferation · γδ T cells · Hydroa vacciniforme

T. Wada (✉) · A. Toga · Y. Sakakibara · T. Toma · A. Yachie
Department of Pediatrics, School of Medicine,
Institute of Medical, Pharmaceutical and Health Sciences,
Kanazawa University, 13-1 Takaramachi,
Kanazawa 920-8641, Japan
e-mail: taizo@staff.kanazawa-u.ac.jp

M. Hasegawa · K. Takehara
Department of Dermatology, School of Medicine,
Institute of Medical, Pharmaceutical and Health Sciences,
Kanazawa University, Kanazawa, Japan

T. Shigemura
Department of Pediatrics, Shinshu University School
of Medicine, Matsumoto, Japan

K. Agematsu
Department of Infection and Host Defense,
Shinshu University School of Medicine, Matsumoto, Japan

Introduction

Epstein–Barr virus (EBV) is a herpes virus that is ubiquitous in the human population. Primary EBV infection occasionally causes infectious mononucleosis that is an acute and usually benign self-limited disease [1]. The target of EBV infection is primarily B lymphocytes. However, EBV infection has also been etiologically associated with various malignancies and lymphoproliferative disorders including chronic active EBV infection (CAEBV), in which monoclonal or oligoclonal proliferation of EBV-infected T or natural killer (NK) cells may play important roles in disease development [2]. CAEBV is characterized by persistent or recurrent infectious mononucleosis-like symptoms such as fever, lymphadenopathy and hepatosplenomegaly, and by extremely high viral loads in peripheral blood [3]. Patients with CAEBV may also suffer from cutaneous lesions including hypersensitivity to mosquito bites or hydroa vacciniforme (HV)-like eruptions. Based on the cellular targets of EBV, CAEBV can be divided into T cell-type and NK cell-type infections [4]. T cell-type CAEBV is further subdivided into $CD4^+$, $CD8^+$, and γδ T cell-type infections.

HV is a rare photosensitivity disorder characterized by vesicle, crust and scar formation on sun-exposed areas with onset in childhood. Although the origin of this condition remains unknown, HV resolves spontaneously by adulthood in most cases [5]. However, there also have been severe cases accompanied by systemic manifestations including fever, lymphadenopathy and liver dysfunction. These patients may progress to cutaneous T cell lymphoma [6]. Accumulating evidence has suggested that both typical and severe HV are associated with latent EBV infection [7–9]. In addition, $\gamma\delta$ T cells have recently been demonstrated to be the major cellular target of EBV infection in HV [10–12]. However, the immunophenotypic features of EBV-infected $\gamma\delta$ T cells and their involvement in skin lesions in CAEBV and/or HV are not fully understood. In this report, we describe 3 patients with CAEBV whose $\gamma\delta$ T cells were predominantly infected by EBV, and show their selective activation, clonal expansion, and recruitment to HV skin lesions.

Materials and methods

Patients

We evaluated 3 Japanese patients with $\gamma\delta$ T cell-type CAEBV. The clinical and immunological data of patient 1 have been reported elsewhere [13]. Patient 2 was a 10-year-old girl who had frequent episodes of fever, stomatitis, and liver dysfunction since the age of 4 years. She had mild hepatosplenomegaly. The copy numbers of the EBV genome were found to be extremely high in the peripheral blood at the age of 9 years (1.2×10^5 copies/μg DNA). There was no history of hypersensitivity to mosquito bites and HV in this patient. Patient 3 was a 14-year-old female who developed vesiculopapules on sun-exposed skin at the age of 4 years. A diagnosis of HV was made at the age of 5 years, when skin biopsy specimens exhibited the presence of EBV genome. The EBV viral loads in the peripheral blood were in the range of 3.5×10^3–5.4×10^4 copies/μg DNA. Despite the absence of hepatosplenomegaly or lymphadenopathy, her clinical history was remarkable for occasional febrile episodes and frequent severe gingivitis in addition to HV. Approval for the study was obtained from the Human Research Committee of Kanazawa University Graduate School of Medical Science, and informed consent was provided according to the Declaration of Helsinki.

Cell preparations and in situ hybridization for EBV-encoded small RNA1 (EBER-1)

Peripheral blood mononuclear cells (PBMCs) were isolated by Ficoll-Hypaque gradient centrifugation from patients and controls. Peripheral blood lymphocytes (PBLs) were prepared from PBMCs by depletion of monocytes using anti-CD14 monoclonal antibody (mAb)-coated magnetic beads. $CD4^+$ T, $CD8^+$ T, $CD19^+$ B, and $CD56^+$ NK cells were then purified by positive selection from PBLs using mAb-coated magnetic beads [14]. To obtain $\gamma\delta$ T cells, PBLs were stained with biotin-conjugated anti-T cell receptor (TCR) $\gamma\delta$ mAb, followed by incubation with streptavidin-coated magnetic beads (all from Becton-Dickinson, San Diego, CA). The purity of the isolated $\gamma\delta$, $CD4^+$, and $CD8^+$ T cells from patient 2 was 95.6, 98.6, and 97.8 %, respectively, as determined by flow cytometric analysis. The purity of the isolated $\gamma\delta$ T, $CD4^+$ T, $CD8^+$ T, $CD19^+$ B, and $CD56^+$ NK cells from patient 3 was 98.2, 98.4, 94.7, 96.2, and 92.8 %, respectively. In situ hybridization for EBER-1 was performed as described previously [14].

Flow cytometry

Expression of Vδ chains and human leukocyte antigen (HLA)-DR was evaluated on $\gamma\delta$ T cells using a FACSCalibur flow cytometer with CellQuest software (BD Bioscience, Tokyo, Japan) [14]. The following mAbs were used: fluorescein isothiocyanate-conjugated anti-TCR Vδ1 (Thermo Scientific, Rockford, IL), anti-TCR Vδ2 (Immunotech, Marseille, France), anti-TCR Pan $\gamma\delta$ (Immunotech), and phycoerythrin-labled anti-HLA-DR (Becton-Dickinson).

Analysis of TCR Vδ and Vγ mRNA

Complementarity determining region 3 (CDR3) spectratyping was performed as described previously, with minor modifications [15, 16]. Briefly, each fragment of TCR Vδ and Vδ was amplified from cDNA obtained from PBMCs with one of 3 Vδ-specific or 3 Vγ-specific primers, respectively. Thirty-five or 30 cycles of amplification (94 °C for 45 s, 60 °C for 45 s, and 72 °C for 45 s) were used, and the polymerase chain reaction (PCR) products were then subjected to run-off reactions using a nested 6-fluorescein phosphoramidite-labelled Cδ or Cγ primer, respectively. The size distribution of each of the fluorescent PCR products was determined as described previously [17]. Quantitative reverse-transcription (RT)-PCR of TCR Vδ2 was performed on an ABI 7700 Sequence Detection System (Applied Biosystems, Foster City, CA) using the SYBR GreenER qPCR SuperMix for ABI Prism (Invitrogen, Carlsbad, CA) [14]. We used β-actin as the reference gene. The PCR products of Vδ2 cDNA were subcloned with a TOPO TA cloning kit (Invitrogen) and subcloned PCR products were sequenced using the ABI Prism BigDye Terminator Cycle Sequencing Kit on an ABI 3100 automated sequencer (Applied Biosystems).

Analysis of TCR Vδ genomic sequences in skin

TCR-δ gene rearrangements were detected by family-specific multiplex PCR, as described previously [18]. Genomic DNA extracted from paraffin-embedded skin biopsy specimens with DEXPAT (Takara Bio Inc., Shiga, Japan) was subjected to PCR amplification using 6 TCR Vδ-specific forward primers and 4 TCR Jδ-specific reverse primers that could detect all major Dδ(D)Jδ rearrangements. PCR products were then subcloned and sequenced.

Results

Ectopic EBV infection of γδ T cells

To determine which populations of lymphocytes were infected with EBV, in situ hybridization for EBER-1 was performed on samples isolated from the patients. As shown in Fig. 1, γδ T cells were found to account for the majority of EBER-1$^+$ cells, with negligible EBER-1 identified in CD4$^+$ T, CD8$^+$ T, CD19$^+$ B, and CD56$^+$ NK cells in all cases. Immunophenotypic analysis of lymphocyte subsets exhibited markedly increased percentages of γδ T cells in their peripheral blood (Fig. 2a). More than 80 % of those γδ T cells expressed the activation marker HLA-DR, which is generally negative in normal γδ T cells (Fig. 2b). The ratio of CD4$^+$ to CD8$^+$ T cells and the percentage expression of CD45RO$^+$ memory marker in CD4$^+$ and CD8$^+$ T cells were normal in all patients (data not shown).

Clonal expansion of Vγ9$^+$ Vδ2$^+$ γδ T cells

We next analyzed the diversity of the TCR Vδ repertoire in γδ T cells from the patients using Vδ-specific mAbs and CDR3 spectratyping. Flow cytometric analysis clearly demonstrated a massive expansion of TCR Vδ2$^+$ cells among the γδ T cells from these patients (Fig. 2a). In age-matched controls, CDR3 spectratyping of the TCR Vδ1, δ2, and δ3 segments exhibited a Gaussian curve reflecting the polyclonal Vδ repertoire (Fig. 3a). Although all 3 Vδ segments were amplified from the patients' cDNA, preferential usage of TCR Vδ2 was seen on their gel images in the patients compared with

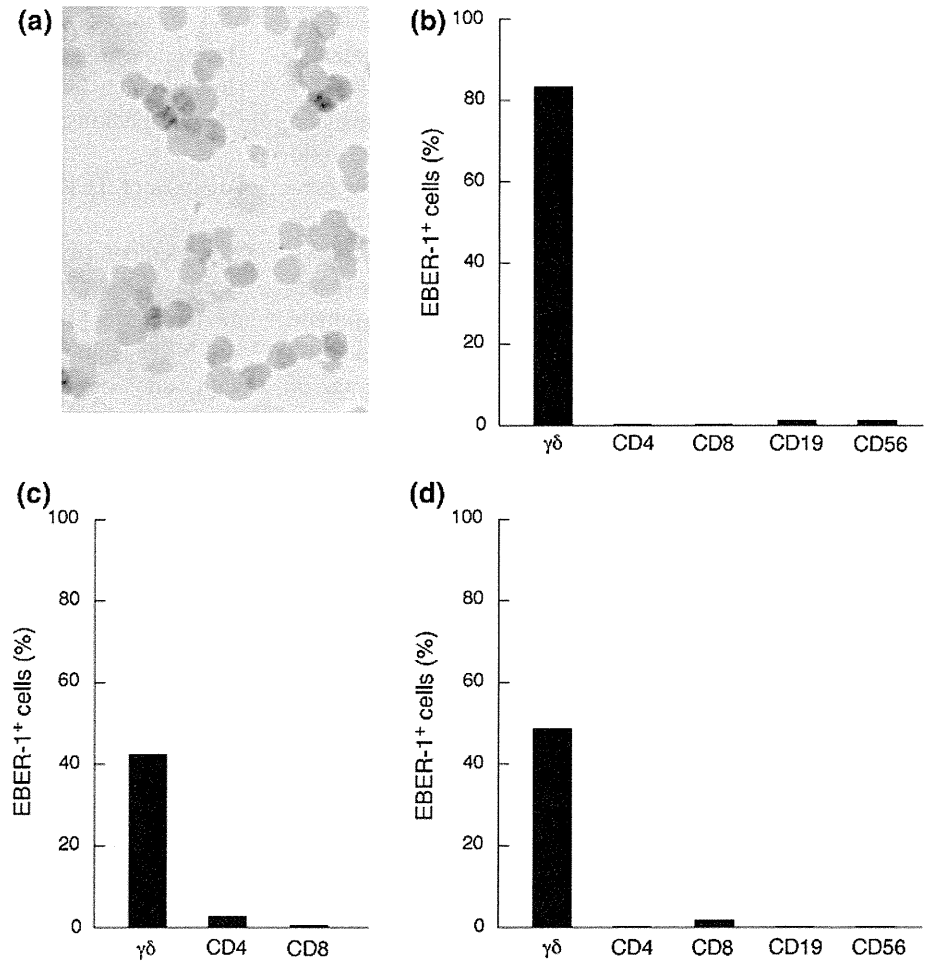

Fig. 1 Characterization of EBV-infected cells. **a** Detection of EBER-1$^+$ cells in γδ T cells from patient 3. **b–d** Frequency of EBV-infected cells. The percentage of EBER-1$^+$ cells within the patients' lymphocyte subsets are shown in patient 1 (**b**), patient 2 (**c**), and patient 3 (**d**)

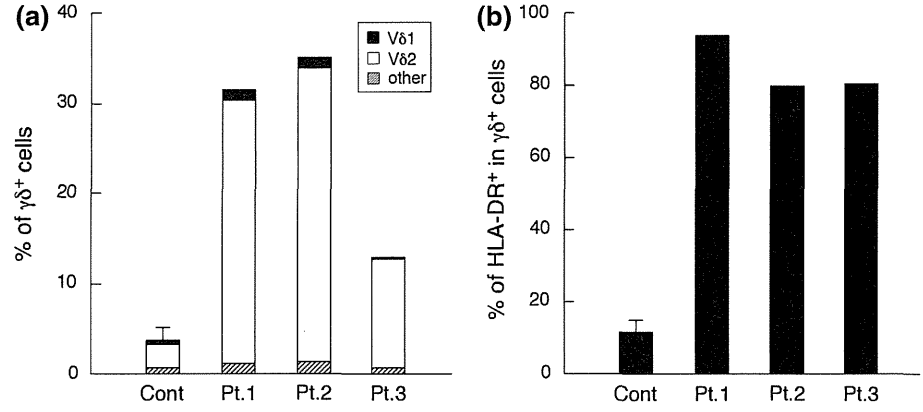

Fig. 2 Immunophenotype of $\gamma\delta$ T cells. **a** Expression profiles of T cell receptor (TCR) Vδ subfamilies. Peripheral blood samples were stained with mAbs for anti-TCR Vδ1 or anti-TCR Vδ2 together anti-TCR Pan $\gamma\delta$ mAb. The percentage of cells was analyzed by flow cytometry and expressed with respect to the total lymphocyte population. **b** Activation status of $\gamma\delta$ T cells. Expression of HLA-DR was evaluated in $\gamma\delta$ T cells

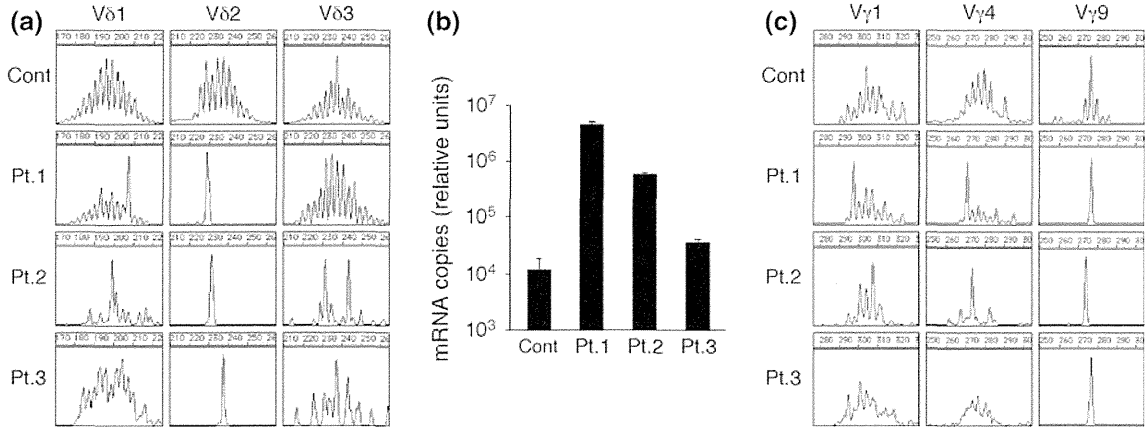

Fig. 3 CDR3 spectratyping and TCR Vδ2 mRNA copies. **a** CDR3 size distribution of TCR Vδ. Each TCR Vδ fragment was amplified from the cDNA with specific primers. The size distribution of the polymerase chain reaction (PCR) products was determined by an automated sequencer and GeneScan software. **b** TCR Vδ2 mRNA was determined by real-time quantitative RT-PCR. Data were normalized to β-actin expression and represent the mean ± SD of 3 independent experiments. **c** CDR3 size distribution of TCR Vγ. Each TCR Vγ fragment was amplified from the cDNA with specific primers

controls (data not shown). Quantitative RT-PCR analysis showed that the levels of Vδ2 mRNA in PBMCs from the patients were much higher than those in PBMCs from controls (Fig. 3b). CDR3 spectratyping of their TCR Vδ2 segments exhibited a single peak, whereas their Vδ1 and Vδ3 segments exhibited polyclonal peaks (Fig. 3a). The junctional amino acid sequence of their TCR Vδ2 segments also exhibited monoclonal profiles (Table 1). The clonally expanded $\gamma\delta$ T cells of patients 1, 2 and 3 were Vδ2-Jδ2$^+$, Vδ2-Jδ1$^+$, Vδ2-Jδ3$^+$ cells, respectively. We also analyzed mRNA of TCR Vγ1, Vγ4 and Vγ9. Similar to those found in TCR Vδ2, the patients' TCR Vγ9 segments were preferentially amplified (data not shown), and showed monoclonal profiles (Fig. 3c). Consistent with these monoclonal TCR Vδ2 and Vγ9 patterns, Southern blot analysis of EBV terminal repeats showed monoclonal EBV in the peripheral blood from all patients (data not shown).

Skin infiltration of Vδ2$^+$ $\gamma\delta$ T cells

The availability of skin biopsy specimens from patient 1 offered us the unique opportunity to investigate whether the clonally expanded $\gamma\delta$ T cells existed in the HV-like eruptions. Although the Vδ clones obtained from her skin lesion included only Vδ2, the Vδ2 segments exhibited a couple of different Jδ. Of note, we were able to show that one of those Vδ2 clones were identical to that of the clonally expanded Vδ2-Jδ2$^+$ $\gamma\delta$ T cells in the peripheral blood (Fig. 4; Table 1). These results suggested that EBV-infected Vδ2$^+$ $\gamma\delta$ T cells infiltrated into the skin lesion.

Discussion

HV has been recently reported to be pathogenically associated with chronic latent EBV infection [7–9]. It is also

Table 1 Junctional amino acid sequences of γδ T cells

	DV	N-D-N	DJ	Frequency
PBMCs, Vδ2				
Control	YCACD	SLNRGTSRD	TDKLIFGKGTRVTVEPR	1/18
	YCACD	TVGGPD	YTDKLIFGKGTRVTVEPR	1/18
	YCACDT	GFGGILS	SWDTRQMFFGTGIKLFVEPR	1/18
	YCACD	SLGDTPP	YTDKLIFGKGTRVTVEPR	1/18
	YCACDT	VGGSVPES	YTDKLIFGKGTRVTVEPR	1/18
	YCAC	EPLGGGYY	YTDKLIFGKGTRVTVEPR	1/18
	YCACDT	LQ	YTDKLIFGKGTRVTVEPR	1/18
	YCACD	TVRGSVLGDTL	TDKLIFGKGTRVTVEPR	1/18
	YCACD	IWGNA	DKLIFGKGTRVTVEPR	1/18
	YCACD	ILGTGA	DKLIFGKGTRVTVEPR	1/18
	YCAC	VGLGAH	DKLIFGKGTRVTVEPR	1/18
	YCACDT	VELGDPTV	TDKLIFGKGTRVTVEPR	1/18
	YCACD	PVGVT	YTDKLIFGKGTRVTVEPR	1/18
	YCACD	FILTRGIS	KLIFGKGTRVTVEPR	1/18
	YCACD	PLRTGGHS	DKLIFGKGTRVTVEPR	1/18
	YCACD	TAGRA	YTDKLIFGKGTRVTVEPR	1/18
	YCAC	VPLLGNH	DKLIFGKGTRVTVEPR	1/18
	YCACD	LLGDDEGY	KLIFGKGTRVTVEPR	1/18
Patient 1	YCACD	ILGD	MTAQLFFGKGTQLIVEPG	24/24
Patient 2	YCACD	SLTGGF	TDKLIFGKGTRVTVEPR	25/27
	YCACD	SLAGGF	TDKLIFGKGTRVTVEPR	1/27
	YCACG	SLTGGF	TDKLIFGKGTRVTVEPR	1/27
Patient 3	YCACD	TGGYA	SWDTRQMFFGTGIKLFVEPR	27/30
	YCACD	TGGYA	SWDARQMFFGTGIKLFVEPR	1/30
	YCACD	TGGYA	SWDTRQMLFGTGIKLFVEPR	1/30
	YCACD	TGGYA	SWDTRQMFIGTGIKLFVEPR	1/30
Skin, Vδ2-Jδ2				
Patient 1	YCACD	ILGD	MTAQLFFGKGTQLIVE	12/12

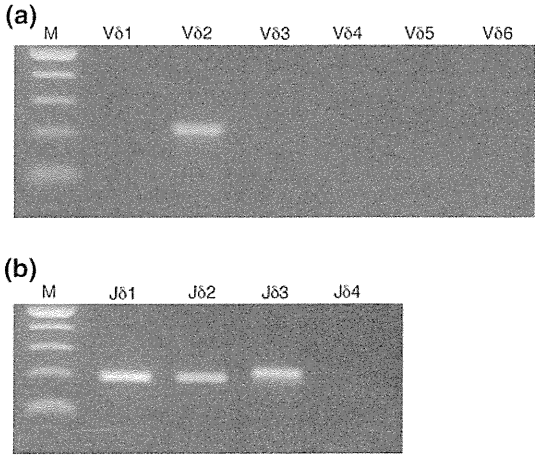

Fig. 4 TCR Vδ genomic sequences in the skin lesion from patient 1. **a** Each TCR Vδ fragment was amplified from skin DNA with one of 6 TCR Vδ-specific forward primers and a combination of 4 TCR Jδ-specific reverse primers. (B) Each TCR Jδ fragment was amplified with the TCR Vδ2-specific forward primer and one of 4 TCR Jδ-specific reverse primers. Lane *M* 100-bp molecular marker

known that patients with CAEBV may present with various cutaneous manifestations including HV-like eruptions [3]. CAEBV patients with HV-like eruptions sometimes develop cutaneous T cell lymphoma that is defined as HV-like lymphoma in the 2008 World Health Organization classification of lymphoid neoplasms [19]. This condition is increasingly being described in children and adolescents from Asia or Latin America [19]. In these diseases, the EBV infection is usually thought to occur in T or NK cells, however, precise immunophenotyping and clonality of those cells remains to be elucidated [7–9].

In the present study, we demonstrated ectopic EBV infection of γδ T cells and increased subpopulations of γδ T cells in the peripheral blood in 3 patients with CAEBV. Interestingly, two of them showed HV-like eruptions. These results were in agreement with recent studies that demonstrated associations between HV and increased numbers of EBV-infected γδ T cells [10–12]. In addition, we found that circulating γδ T cells were in a highly

activated state in our patients. In normal individuals, $\gamma\delta$ T cells usually comprise a small proportion of the circulating lymphocyte population. Expansion of the $\gamma\delta$ T cell subset has been also documented in the context of various infections including *Mycobacterium* and cytomegalovirus [20]. However, selective activation and expansion of $\gamma\delta$ T cells may provide us with clinical clues to suspect ectopic EBV infection of $\gamma\delta$ T cells in children suffering from HV or lymphoproliferative disease. Further investigations are necessary to clarify the major cellular targets of EBV infection and to understand the pathophysiological link between ectopic EBV infection and the clinical manifestations of the disease.

There was clear evidence of clonal expansion of $V\gamma9^+$ $V\delta2^+$ $\gamma\delta$ T cells in our patients. We assume that the EBV infection predominantly targeted $V\gamma9^+$ $V\delta2^+$ $\gamma\delta$ T cells and expanded clonally in the patients. Human $\gamma\delta$ T cells exhibit a restricted repertoire using a limited set of $V\gamma$ and $V\delta$ gene elements compared with $\alpha\beta$ T cells. There are only 6 functional $V\gamma$ and 8 functional $V\delta$ genes in human [21]. At birth, the repertoire of $\gamma\delta$ T cells in cord blood is broad with no apparent restriction [22]. However, the initially small subset of $V\gamma9^+$ $V\delta2^+$ cells has been shown to gradually increase with age, resulting in a high frequency of polyclonal $V\gamma9^+$ $V\delta2^+$ cells in adult peripheral blood [23]. Although careful interpretation of the results of monotypic $V\gamma9/V\delta2$ domain expression is needed, in our cases the predominance of $V\gamma9^+$ $V\delta2^+$ $\gamma\delta$ T cell was not likely to be age-dependent. The absolute counts of $V\delta2^+$ $\gamma\delta$ T cells, as well as the $V\delta2$ mRNA levels, in PBMCs were strikingly elevated in our young patients. CDR3 spectratyping of their $V\delta2$ segments showed monoclonal peaks that were confirmed by sequence analysis. In addition, Southern blot analysis of EBV terminal repeats indicated monoclonal EBV infection. On the other hand, studies of T cell lines established from 3 patients with nasal T cell lymphoma or CAEBV have also indicated preferential expansion of EBV-infected $V\gamma9/V\delta2$ $\gamma\delta$ T cells [24]. However, these and our results are insufficient to allow us to draw any conclusion regarding higher susceptibility to EBV infection of $V\gamma9^+$ $V\delta2^+$ $\gamma\delta$ T cells compared with other $\gamma\delta$ T cells. Frequent identification of EBV-infected $V\gamma9^+$ $V\delta2^+$ $\gamma\delta$ T cells could simply be due to a higher percentage of $V\gamma9/V\delta2$ $\gamma\delta$ T cells at the time of infection. The mechanism underlying the ectopic infection also remains elusive.

In patient 1, we have previously demonstrated that approximately 25 % of the cells infiltrating into the HV-like eruptions were EBV positive by in situ hybridization for EBER-1, and that about 30 % of the infiltrating cells appeared to be $CD3^+$ $CD4^-$ $CD8^-$ T cells by immunohistochemical analysis [13]. However, the presence of EBV-infected $\gamma\delta$ T cells in the skin could not be confirmed because of the lack of a suitable anti-TCR $\gamma\delta$ antibody for paraffin-embedded tissues. In the present study, our molecular analysis clearly demonstrated the skin infiltration of $V\delta2^+$ $\gamma\delta$ T cells, which were identical to the clonally expanded $V\delta2^+$ $\gamma\delta$ T cells in the peripheral blood and were thus infected by EBV in this patient. In normal individuals, $\gamma\delta$ T cells take residence mainly in epithelial tissues, such as skin, and represent the major T cell population there, and modulate epithelial homeostasis through their cytokine secretion and cytolytic properties [25]. It is well known that skin lesions of HV can be induced by repeated ultraviolet exposure [26]. Studies in a murine model for drug-induced cutaneous lupus erythematosus demonstrated that ultraviolet might enhance the function of skin $\gamma\delta$ T cells that were involved in skin lesions [27]. Therefore, EBV-infected $\gamma\delta$ T cells may play an important role in the skin lesions of HV. Additional investigation will be required to assess whether the presence of EBV-infected $\gamma\delta$ T cells in the skin lesions results from ectopic EBV infection into skin-resident $\gamma\delta$ T cells or migration of EBV-infected $\gamma\delta$ T cells from peripheral blood after sun exposures.

In summary, our studies demonstrate clonal expansion of EBV-infected $\gamma\delta$ T cells in $\gamma\delta$ T cell-type CAEBV, further support the association between EBV-infected $\gamma\delta$ T cells and HV, and provide the basis for characterization of EBV-infected cells to better understand pathogenesis of EBV-associated lymphoproliferative disorders.

Acknowledgments We thank Ms Harumi Matsukawa and Ms. Shizu Kouraba for their excellent technical assistance. This work was supported by a grant from Takeda Science Foundation, Osaka; a Grant-in-Aid for Scientific Research from the Ministry of Education, Culture, Sports, Science and Technology of Japan; and a grant from the Ministry of Health, Labour, and Welfare of Japan, Tokyo.

Conflict of interest The authors declare that they have no conflict of interest.

References

1. Hislop AD, Taylor GS, Sauce D, Rickinson AB. Cellular responses to viral infection in humans: lessons from Epstein–Barr virus. Annu Rev Immunol. 2007;25:587–617.
2. Cohen JI, Kimura H, Nakamura S, Ko YH, Jaffe ES. Epstein–Barr virus-associated lymphoproliferative disease in non-immunocompromised hosts: a status report and summary of an international meeting, 8–9 September 2008. Ann Oncol. 2009;20:1472–82.
3. Okano M, Kawa K, Kimura H, Yachie A, Wakiguchi H, Maeda A, Imai S, Ohga S, Kanegane H, Tsuchiya S, Morio T, Mori M, Yokota S, Imashuku S. Proposed guidelines for diagnosing chronic active Epstein–Barr virus infection. Am J Hematol. 2005;80:64–9.
4. Kimura H, Hoshino Y, Hara S, Sugaya N, Kawada J, Shibata Y, Kojima S, Nagasaka T, Kuzushima K, Morishima T. Differences

between T cell-type and natural killer cell-type chronic active Epstein–Barr virus infection. J Infect Dis. 2005;191:531–9.
5. Gupta G, Man I, Kemmett D. Hydroa vacciniforme: a clinical and follow-up study of 17 cases. J Am Acad Dermatol. 2000;42: 208–13.
6. Chen HH, Hsiao CH, Chiu HC. Hydroa vacciniforme-like primary cutaneous CD8-positive T-cell lymphoma. Br J Dermatol. 2002;147:587–91.
7. Iwatsuki K, Xu Z, Takata M, Iguchi M, Ohtsuka M, Akiba H, Mitsuhashi Y, Takenoshita H, Sugiuchi R, Tagami H, Kaneko F. The association of latent Epstein–Barr virus infection with hydroa vacciniforme. Br J Dermatol. 1999;140:715–21.
8. Cho KH, Lee SH, Kim CW, Jeon YK, Kwon IH, Cho YJ, Lee SK, Suh DH, Chung JH, Yoon TY, Lee SJ. Epstein–Barr virus-associated lymphoproliferative lesions presenting as a hydroa vacciniforme-like eruption: an analysis of six cases. Br J Dermatol. 2004;151:372–80.
9. Iwatsuki K, Satoh M, Yamamoto T, Oono T, Morizane S, Ohtsuka M, Xu ZG, Suzuki D, Tsuji K. Pathogenic link between hydroa vacciniforme and Epstein–Barr virus-associated hematologic disorders. Arch Dermatol. 2006;142:587–95.
10. Kimura H, Miyake K, Yamauchi Y, Nishiyama K, Iwata S, Iwatsuki K, Gotoh K, Kojima S, Ito Y, Nishiyama Y. Identification of Epstein–Barr virus (EBV)-infected lymphocyte subtypes by flow cytometric in situ hybridization in EBV-associated lymphoproliferative diseases. J Infect Dis. 2009;200:1078–87.
11. Kimura H, Ito Y, Kawabe S, Gotoh K, Takahashi Y, Kojima S, Naoe T, Esaki S, Kikuta A, Sawada A, Kawa K, Ohshima K, Nakamura S. EBV-associated T/NK-cell lymphoproliferative diseases in nonimmunocompromised hosts: prospective analysis of 108 cases. Blood. 2012;119:673–86.
12. Hirai Y, Yamamoto T, Kimura H, Ito Y, Tsuji K, Miyake T, Morizane S, Suzuki D, Fujii K, Iwatsuki K. Hydroa vacciniforme is associated with increased numbers of Epstein–Barr virus-infected γδ T Cells. J Invest Dermatol. 2012;132:1401–8.
13. Tanaka C, Hasegawa M, Fujimoto M, Iwatsuki K, Yamamoto T, Yamada K, Kawa K, Saikawa Y, Toga A, Mase S, Wada T, Takehara K, Yachie A. Phenotypic analysis in a case of hydroa vacciniforme-like eruptions associated with chronic active Epstein–Barr virus disease of γδ T cells. Br J Dermatol. 2012; 166:216–8.
14. Toga A, Wada T, Sakakibara Y, Mase S, Araki R, Tone Y, Toma T, Kurokawa T, Yanagisawa R, Tamura K, Nishida N, Taneichi H, Kanegane H, Yachie A. Clinical significance of cloned expansion and CD5 down-regulation in Epstein–Barr virus (EBV)-infected CD8+ T lymphocytes in EBV-associated hemophagocytic lymphohistiocytosis. J Infect Dis. 2010;201: 1923–32.
15. de Villartay JP, Lim A, Al-Mousa H, Dupont S, Dechanet-Merville J, Coumau-Gatbois E, Gougeon ML, Lemainque A, Eidenschenk C, Jouanguy E, Abel L, Casanova JL, Fischer A, Le Deist F. A novel immunodeficiency associated with hypomorphic RAG1 mutations and CMV infection. J Clin Invest. 2005;115: 3291–9.
16. Ehl S, Schwarz K, Enders A, Duffner U, Pannicke U, Kuhr J, Mascart F, Schmitt-Graeff A, Niemeyer C, Fisch P. A variant of SCID with specific immune responses and predominance of γδ T cells. J Clin Invest. 2005;115:3140–8.
17. Wada T, Schurman SH, Otsu M, Garabedian EK, Ochs HD, Nelson DL, Candotti F. Somatic mosaicism in Wiskott–Aldrich syndrome suggests in vivo reversion by a DNA slippage mechanism. Proc Natl Acad Sci USA. 2001;98:8697–702.
18. van Dongen JJ, Langerak AW, Bruggemann M, Evans PA, Hummel M, Lavender FL, Delabesse E, Davi F, Schuuring E, Garcia-Sanz R, van Krieken JH, Droese J, Gonzalez D, Bastard C, White HE, Spaargaren M, Gonzalez M, Parreira A, Smith JL, Morgan GJ, Kneba M, Macintyre EA. Design and standardization of PCR primers and protocols for detection of clonal immunoglobulin and T-cell receptor gene recombinations in suspect lymphoproliferations: report of the BIOMED-2 Concerted Action BMH4-CT98-3936. Leukemia. 2003;17:2257–317.
19. Quintanilla-Martinez L KH, Jaffe ES. EBV-positive T-cell lymphoproliferative disorders of childhood. Geneva, Switzerland: World Health Organization, 2008.
20. Dechanet J, Merville P, Lim A, Retiere C, Pitard V, Lafarge X, Michelson S, Meric C, Hallet MM, Kourilsky P, Potaux L, Bonneville M, Moreau JF. Implication of γδ T cells in the human immune response to cytomegalovirus. J Clin Invest. 1999;103: 1437–49.
21. O'Brien RL, Roark CL, Jin N, Aydintug MK, French JD, Chain JL, Wands JM, Johnston M, Born WK. γδ T-cell receptors: functional correlations. Immunol Rev. 2007;215:77–88.
22. Morita CT, Parker CM, Brenner MB, Band H. TCR usage and functional capabilities of human gamma delta T cells at birth. J Immunol. 1994;153:3979–88.
23. Parker CM, Groh V, Band H, Porcelli SA, Morita C, Fabbi M, Glass D, Strominger JL, Brenner MB. Evidence for extrathymic changes in the T cell receptor gamma/delta repertoire. J Exp Med. 1990;171:1597–612.
24. Oyoshi MK, Nagata H, Kimura N, Zhang Y, Demachi A, Hara T, Kanegane H, Matsuo Y, Yamaguchi T, Morio T, Hirano A, Shimizu N, Yamamoto K. Preferential expansion of Vγ9-JγP/ Vδ2-Jδ3 γδ T cells in nasal T-cell lymphoma and chronic active Epstein–Barr virus infection. Am J Pathol. 2003;162:1629–38.
25. Komori HK, Meehan TF, Havran WL. Epithelial and mucosal gamma delta T cells. Curr Opin Immunol. 2006;18:534–8.
26. Verneuil L, Gouarin S, Comoz F, Agbalika F, Creveuil C, Varna M, Vabret A, Janin A, Leroy D. Epstein–Barr virus involvement in the pathogenesis of hydroa vacciniforme: an assessment of seven adult patients with long-term follow-up. Br J Dermatol. 2010;163:174–82.
27. Yoshimasu T, Nishide T, Seo N, Hiroi A, Ohtani T, Uede K, Furukawa F. Susceptibility of T cell receptor-alpha chain knockout mice to ultraviolet B light and fluorouracil: a novel model for drug-induced cutaneous lupus erythematosus. Clin Exp Immunol. 2004;136:245–54.

Mod Rheumatol (2013) 23:28–35
DOI 10.1007/s10165-012-0630-0

ORIGINAL ARTICLE

Serum amyloid A (SAA) induces pentraxin 3 (PTX3) production in rheumatoid synoviocytes

Kenshi Satomura · Takafumi Torigoshi · Tomohiro Koga · Yumi Maeda · Yasumori Izumi · Yuka Jiuchi · Taiichiro Miyashita · Satoshi Yamasaki · Atsushi Kawakami · Yoshihiro Aiba · Minoru Nakamura · Atsumasa Komori · Junji Sato · Hiromi Ishibashi · Satoru Motokawa · Kiyoshi Migita

Received: 17 August 2011 / Accepted: 28 February 2012 / Published online: 24 March 2012

Abstract
Objective Pentraxin 3 (PTX3) is an acute-phase reactant that is involved in amplification of the inflammatory response and innate immunity. In the present study, we evaluated the relationship between PTX3 and serum amyloid A (SAA), another acute-phase reactant, in rheumatoid synoviocytes.
Methods PTX3 mRNA expression was examined by reverse transcription polymerase chain reaction, and PTX3 protein was measured by enzyme-linked immunosorbent assay.
Results SAA induced PTX3 mRNA and PTX3 protein expression in rheumatoid synoviocytes. SAA-induced PTX3 expression was attenuated when rheumatoid synoviocytes were nucleofected with *N*-formyl peptide receptor ligand-1 (FPRL-1)-specific siRNA, suggesting the involvement of FPRL-1. Furthermore, SAA-induced PTX3 expression was inhibited by NF-κB or mitogen-activated protein kinase-specific inhibitors. Neither soluble TNF receptor (etanercept) nor recombinant IL-1 receptor antagonist affected PTX3 production by SAA-stimulated synoviocytes, suggesting that SAA directly induces PTX3.
Conclusion Our data suggest that SAA plays a role in the proinflammatory and immune responses in rheumatoid synovium by inducing PTX3. We provide the first evidence that the acute-phase reactant SAA, which is produced systemically by hepatocytes, perpetuates the rheumatoid inflammatory processes by inducing another proinflammatory molecule, PTX3, locally in rheumatoid synovial tissues.

Keywords Pentraxin 3 · Rheumatoid arthritis · Serum amyloid A · Synoviocytes

K. Satomura · T. Torigoshi · Y. Izumi · T. Miyashita · S. Motokawa · K. Migita
Department of Rheumatology, Nagasaki Medical Center, Omura, Nagasaki 856-8562, Japan

K. Satomura · T. Torigoshi · S. Motokawa
Department of Orthopedic Surgery, Nagasaki Medical Center, Omura, Nagasaki 856-8562, Japan

T. Koga · S. Yamasaki · A. Kawakami
Department of Rheumatology, Nagasaki University Hospital, Nagasaki, Japan

Y. Maeda · Y. Jiuchi · Y. Aiba · M. Nakamura · A. Komori · H. Ishibashi · K. Migita (✉)
Clinical Research Center, NHO Nagasaki Medical Center, Kubara 2-1001-1, Omura, Nagasaki 856-8562, Japan
e-mail: migita@nmc.hosp.go.jp

J. Sato
Research and Development Division, Eiken Chemical Co. Ltd, Nogi, Tochigi, Japan

Introduction

Pentraxins are a family of proteins considered to be markers of acute-phase inflammation [1]. C-reactive protein (CRP) and serum amyloid P component (SAP) are members of the short pentraxins, which are produced in the liver in response to inflammatory mediators [2]. Pentraxin 3 (PTX3) is a long pentraxin that is structurally related to but distinct from short pentraxins [3]. PTX3 also differs from these short pentraxins in term of gene organization, cellular expression, and the signaling pathways responsible for their induction [4]. PTX3 is produced in response to proinflammatory signals (i.e., bacterial products, IL-1, TNF, but not IL-6) in diverse cell types, primarily including macrophages and endothelial cells, but not

hepatocytes [5]. PTX3 regulates inflammatory responses and innate immunity [6]. This is supported by studies showing that PTX3 binds to the C1q component of the complement cascade and participates in the clearance of apoptotic cells [7]. PTX3 is elevated in patients with systemic inflammation, such as septic shock, myocardial infarction, systemic vasculitis, and rheumatoid arthritis (RA) [8–11].

Serum amyloid A (SAA) is another acute-phase reactant that is produced by hepatocytes [12]. A number of immunomodulatory roles of SAA have been reported to exhibit cytokine-like properties [13]. SAA has been demonstrated to be a chemotactic ligand for the human *N*-formyl peptide receptor ligand-1 (FPRL-1), a transmembrane G-protein-coupled receptor [14]. SAA can act as a chemoattractant for monocytes and T lymphocytes [15]. Furthermore, SAA can stimulate the secretion of the proinflammatory cytokines IL-1, IL-6, IL-8, and TNF-α [16].

Rheumatoid arthritis is a chronic inflammatory disease that is characterized by synovitis and cartilage destruction. Elevated levels of SAA are observed in the sera, synovial fluids, and inflamed synovium from RA patients [17]. Considering the numerous biological functions of PTX3 and SAA, the interactions between these acute-phase reactants in rheumatoid synovium should be investigated. The aim of the present study was to evaluate whether PTX3 expression is modulated through interaction with another acute-phase reactant, SAA, in the rheumatoid synovium.

Methods

Patients

All RA patients fulfilled the American College of Rheumatology criteria for RA. Synovial tissue samples were obtained from six patients with RA and a patient with osteoarthritis (OA). Synoviocytes were isolated from the synovial tissues by enzymatic digestion. The isolated synoviocytes were used at the third or fourth passages for all subsequent experiments. The whole study was approved by the Ethics Committees Nagasaki Medical Center, and informed consent was obtained from each of the individuals.

Reagents

Recombinant human SAA was purchased from Peprotech (Rocky Hills, NJ, USA). Polymyxin B and human high-density lipoprotein (HDL) were purchased from Sigma (St. Louis, MO). SB203580, SP600125 and BAY11-7082 were obtained from Calbiochem (San Diego, CA, USA). Recombinant human TNF-α and IL-1β were purchased from R&D Systems (Minneapolis, MN, USA). Recombinant human interleukin-1 receptor antagonist (IL-1ra) was purchased from IMGENEX (San Diego, CA, USA).

Immunohistochemistry

For immunohistochemical analysis for SAA, formalin-fixed and paraffin-embedded tissue blocks were cut into 4 μm thick sections. The sections were deparaffinized in xylene and subsequently rehydrated in sequential ethanol (100–70 %). After washing 3 times with 10 mmol/L phosphate-buffered saline (PBS) (pH 7.4), antigen retrieval was performed by first heating in a microwave at 95 °C for 20 min and then washing twice in PBS for 10 min. The sections were treated with peroxidase-blocking solution (DAKO Japan, Kyoto, Japan) for 5 min, and incubated with 1:1000 dilution of rabbit anti-SAA polyclonal antibody. A standardized two-step method with ENVISION plus (DAKO) was used for detection. The reaction products were visualized using diaminobenzidine as a chromogen (DAKO), and counterstained with Mayer's hematoxylin (DAKO).

Reverse transcription polymerase chain reaction (RT-PCR)

Total cellular RNA was extracted with Trizol (Invitrogen, Carlsbad, CA, USA) according to the manufacturer's protocol. First-strand cDNA was synthesized from 1 μg of total cellular RNA using an RNA PCR kit (Takara Bio Inc., Otsu, Japan) with random primers. Thereafter, cDNA was amplified using specific primers for PTX3 or β-actin, respectively. The specific primers used were as follows [18]:

PTX3: forward primer 5′-CATCCAGTGAGACCAATGAG-3′, reverse primer 5′-GTAGCCGCCAGTTCACCATT-3′

β-actin: forward primer 5′-GTGGGGCGCCCCAGGCACCA-3′, reverse primer 5′-CTCCTTAATGTCACGCACGATTTC-3′

The product sizes were 279 bp for PTX3 and 234 bp for β-actin. The thermocycling conditions for the targets were as follows: 30 cycles 95 °C for 60 s and 58 °C for 30 s, and 72 °C for 60 s. The PCR products were electrophoresed on 2 % agarose gels and visualized by ethidium bromide staining.

Measurement of PTX3 secretion

Rheumatoid synoviocytes (5×10^4 cells) were seeded in 24-well plates containing RPMI plus 10 % fetal calf serum and the cells were stimulated with SAA (0–5 μg/mL) for

24 h. Cell-free supernatants were collected by centrifugation at 400×*g* for 5 min and assayed for PTX3 using enzyme-linked immunosorbent assay (ELISA) kits (R&D Systems, Minneapolis, MN, USA) according to the manufacturer's instructions.

siRNA transfection

Rheumatoid synoviocytes (5×10^4 cells) were transfected with FPLR-1 or scrambled negative control Smartpool small interfering RNA (siRNA; Santa Cruz Biotechnology, Santa Cruz, CA, USA), according to the manufacturer's instructions (Santa Cruz).

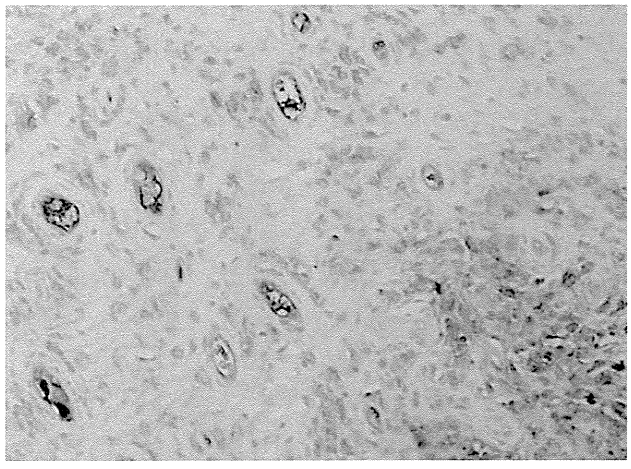

Fig. 1 SAA protein expression in rheumatoid synovial tissues. Rheumatoid synovial tissue sections were stained using antibodies that were specific for SAA protein. SAA was localized in rheumatoid synoviocytes in addition to the endothelial cells. The results are representative of three independent experiments (original magnification ×200)

Western blot analysis

For measurement of FPRL-1 expression by a western blot analysis, si-RNA-treated synoviocytes were washed with ice-cold PBS and lysed with a lysis buffer (1 % Nonidet P 40, 50 mM Tris, pH 7.5, 100 mM NaCl, 50 mM NaF, 5 mM EDTA, 20 mM *β*-glycerophosphate, 1.0 mM sodium orthovanadate, 10 μg/mL aprotinin, and 10 μg/mL leupeptin) for 20 min at 4 °C. Insoluble material was removed by centrifugation at 15,000×*g* for 15 min at 4 °C. The supernatant was saved and the protein concentration was determined using a Bio-Rad protein assay kit (Bio Rad, Hercules, CA, USA). An identical amount of protein (50 μg) for each lysate was subjected to 10 % SDS-polyacrylamide gel electrophoresis and then transferred to a nitrocellulose membrane. Western blot analysis using the primary monoclonal antibodies against FPRL-1 (Santa Cruz Biotechnology, Santa Cruz, CA, USA) or *β*-actin (Sigma, St. Louis, MO, USA) antibodies was performed with an ECL western blotting kit (Amersham, Little Chalfont, UK).

Statistical analysis

Differences between groups were examined for statistical significance using Wilcox's signed rank test. *p* values of less than 0.05 were considered statistically significant.

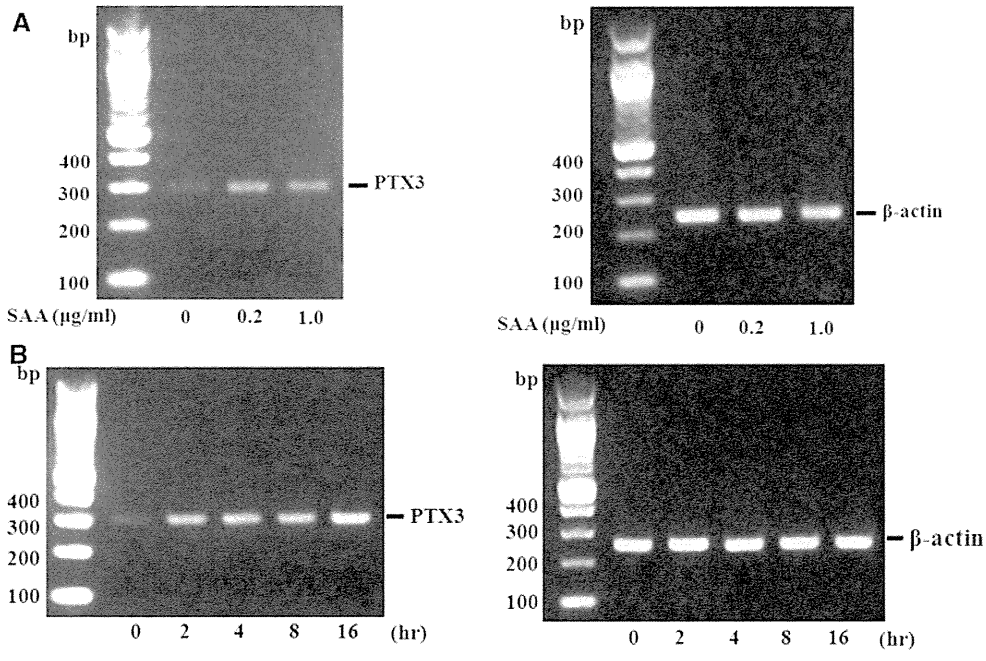

Fig. 2 Semi-quantitative analysis of PTX3 mRNA expression in RA synoviocytes. **a** Rheumatoid synoviocytes were stimulated by SAA for 4 h. Total RNA was analyzed by reverse transcription polymerase chain reaction (RT-PCR) using specific primers for PTX3. *β*-Actin was used as internal control. **b** Rheumatoid synoviocytes were stimulated by SAA (1 μg/mL) for various incubation times. Total RNA was analyzed by reverse transcription polymerase chain reaction (RT-PCR) using primers specific for PTX3. *β*-Actin was used as internal control. The data sare representative of three independent experiments performed using different rheumatoid synoviocytes

Results

Serum amyloid A (SAA) expression in rheumatoid synovium

First, we examined whether rheumatoid synoviocytes express SAA using immunohistochemical techniques. Positive SAA staining was observed in synovial fibroblasts in addition to vascular endothelial cells (Fig. 1).

SAA induces expression of PTX3 in rheumatoid synoviocytes

To evaluate whether SAA can induce PTX3 expression, rheumatoid synoviocytes were stimulated with SAA for 4 h. In primary cultured rheumatoid synoviocytes, PTX3 mRNA expression was barely detectable, whereas PTX3 mRNA expression was induced by SAA stimulation (Fig. 2a). When rheumatoid synoviocytes were stimulated with SAA (1.0 μg/mL) for various time periods (0, 2, 4, 8, 16 h), PTX3 mRNA expression was induced after 2 h of SAA stimulation (Fig. 2b). Verification of the data obtained from RT-PCR (mRNA analysis) by ELISA confirmed that SAA promotes PTX3 protein synthesis in rheumatoid synoviocytes. A minimal dose of 2.0 μg/mL of SAA was sufficient to induce PTX3 protein synthesis (Fig. 3a). SAA-mediated PTX3 induction reached a plateau at physiological concentrations of SAA. The potential effects of contaminating lipopolysaccharide (LPS) in the SAA preparation were examined. SAA was incubated with polymyxin B, an amphiphilic cyclic polycationic peptide that forms a complex with LPS, preventing the biological effects of it. Polymyxin B did not alter the synthesis of PTX3 expression by SAA (Fig. 3b). Under the same experimental conditions, polymyxin B inhibited LPS-induced PTX3 expression.

In RA patients, high levels of IL-1β and TNF-α are present in both synovium and synovial fluids [18]. To reproduce the inflammatory situation in RA synovium, we investigated whether the inflammatory cytokines IL-1β and TNF-α could enhance PTX3 expression in our experimental system. Rheumatoid synoviocytes were incubated with increasing concentrations of IL-1β and TNF-α, in addition to SAA. After 24 h of culture, the supernatants were collected and PTX3 was measured by ELISA. PTX3 secretion was increased by IL-1β and TNF-α in a dose-dependent manner (Fig. 4a). However, SAA-induced PTX3 production was not affected by the addition of IL-1β or TNF-α (Fig. 4b). As shown in Fig. 2b, 16 h of exposure to SAA increased PTX3 mRNA expression, suggesting that the other cytokines, such as TNF-α or IL-1β, which are induced by long exposures to SAA, contribute to the induction of PTX3 mRNA. Therefore, we evaluated whether these cytokines are involved in the SAA-mediated

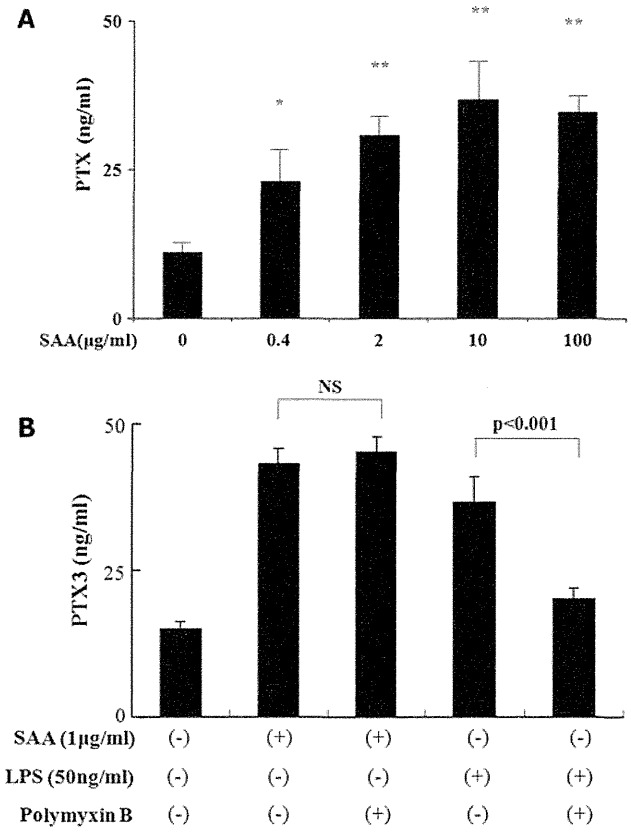

Fig. 3 SAA stimulates PTX3 protein synthesis in RA synoviocytes. **a** Rheumatoid synoviocytes were stimulated with various concentrations of SAA (0–100 μg/mL) as indicated for 24 h under serum-free conditions. PTX3 in the conditioned media was determined by ELISA. The data are representative of two independent experiments performed using different rheumatoid synoviocytes, and are expressed as the mean ± SEM of results obtained in triplicate. $*p < 0.01$ compared to untreated rheumatoid synoviocytes. $**p < 0.001$ compared to untreated rheumatoid synoviocytes. **b** Rheumatoid synoviocytes were stimulated with SAA (1 μg/mL) or lipopolysaccharide (LPS 100 ng/mL) in the presence or absence of polymyxin B (10 μg/mL) for 24 h. PTX3 in the conditioned media was determined by ELISA. The data are representative of three independent experiments performed using different rheumatoid synoviocytes, and are expressed as the mean ± SEM of results obtained in triplicate

PTX3 induction using specific antagonists. As shown in Fig. 4c, neither soluble TNF receptor (etanercept) nor recombinant IL-1 receptor antagonist (IL-1ra) inhibited the PTX3 production of SAA-stimulated synoviocytes, whereas both antagonists completely blocked PTX3 production by TNF-α- or IL-1β-stimulated synoviocytes. These findings suggest that SAA directly induces PTX3 production by synoviocytes.

Circulating SAA is associated with apolipoproteins, such as HDL, which possess some anti-inflammatory properties, as described previously [19]. Therefore, we determined whether HDL would modulate the PTX3-inducing ability of SAA. The addition of HDL at a high concentration of 500 μg/mL resulted in a reduction in the

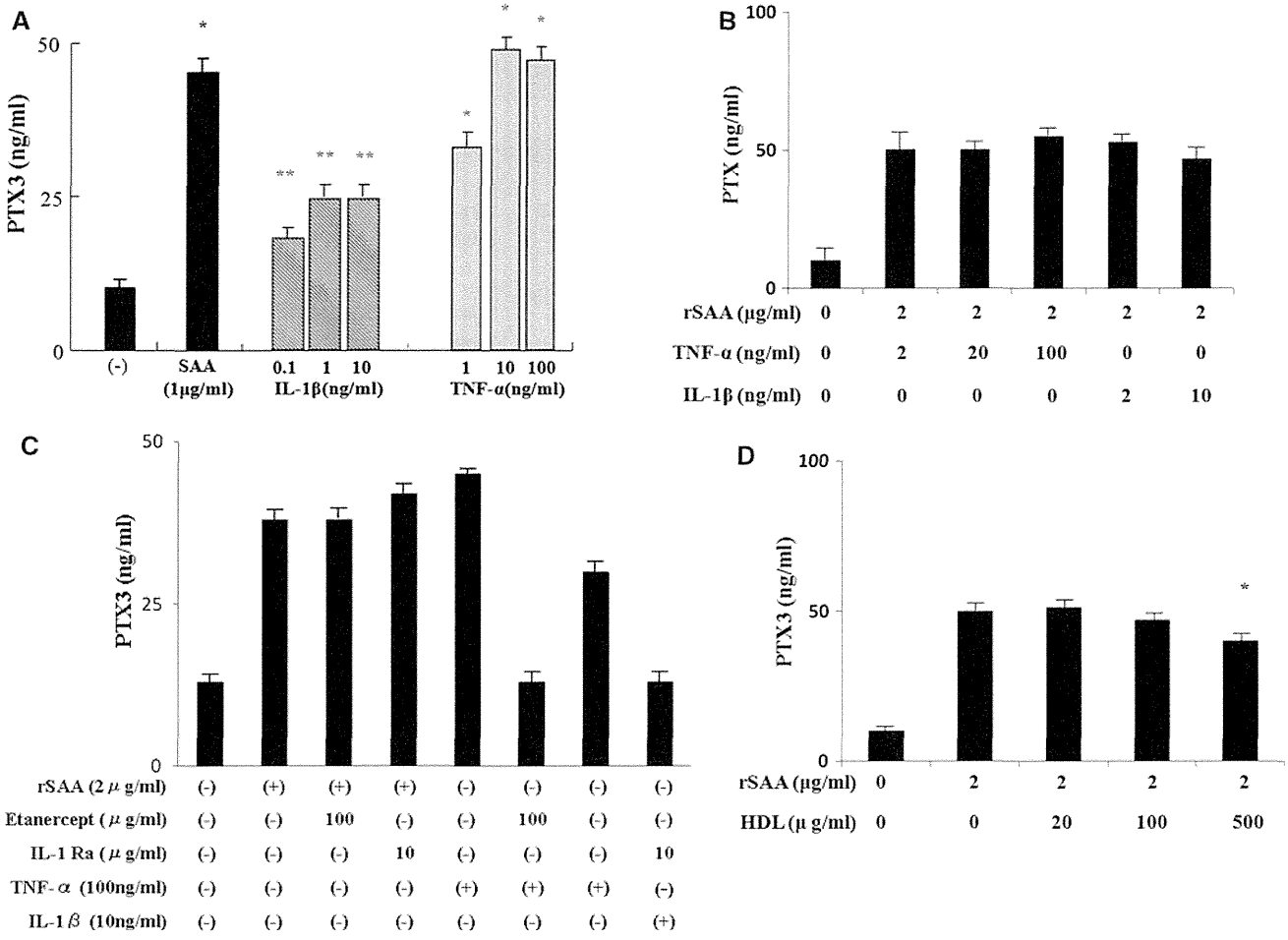

Fig. 4 Effects of IL-1β, TNF-α, and HDL on PTX3 production by rheumatoid synoviocytes. **a** Rheumatoid synoviocytes were cultured with increasing concentrations of IL-1β ($\sim$10 ng/mL), TNF-α ($\sim$100 ng/mL), or SAA (1 μg/mL). After 24 h of culture, PTX3 levels were measured by ELISA. The data are representative of three independent experiments performed using different rheumatoid synoviocytes, are are expressed as the mean ± SEM of results obtained in triplicate. *$p < 0.01$ compared to untreated rheumatoid synoviocytes. **$p < 0.001$ compared to untreated rheumatoid synoviocytes. **b** Rheumatoid synoviocytes were stimulated with SAA in the presence or absence of IL-1β ($\sim$10 ng/mL) or TNF-α ($\sim$100 ng/mL). After 24 h of culture, PTX3 levels were measured by ELISA. The data are representative of three independent experiments performed using different rheumatoid synoviocytes, and are expressed as the mean ± SEM of results obtained in triplicate. **c** Rheumatoid synoviocytes were stimulated with SAA (2 μg/mL), IL-1β (10 ng/mL), or TNF-α (100 ng/mL) in the presence or absence of etanercept or IL-1ra. After 24 h of culture, PTX3 levels were measured by ELISA. The data are representative of two independent experiments performed using different rheumatoid synoviocytes, and are expressed as the mean ± SEM of results obtained in triplicate. **d** Rheumatoid synoviocytes were stimulated with SAA in the presence or absence of HDL ($\sim$500 μg/mL). After 24 h of culture, PTX3 levels were measured by ELISA. The data are representative of three independent experiments performed using different rheumatoid synoviocytes, and are expressed as the mean ± SEM of results obtained in triplicate. *$p < 0.01$ compared to SAA-stimulated rheumatoid synoviocytes. *$p < 0.01$ compared to SAA-treated rheumatoid synoviocytes

PTX3-inducing ability of SAA (Fig. 4d). These findings suggest that SAA-mediated PTX3 induction can be modulated through its interaction with HDL.

Role of NF-κB and MAPKs in SAA-induced expression of PTX3

Previously, we demonstrated that SAA induced the activation of NF-κB and MAPKs (p38, JNK) in rheumatoid synoviocytes [20]. To determine the involvement of these signaling molecules in the SAA-mediated induction of PTX3, rheumatoid synoviocytes were pretreated with the specific inhibitors SB203580 (p38), SP600125 (JNK), and Bay11-7082 (NF-κB). As shown in Fig. 5, inhibition of the NF-κB, p38, or JNK MAPK signaling pathways led to substantial reductions in SAA-induced PTX3 synthesis.

FPRL-1 downregulation leads to the suppression of PTX3 expression from SAA-treated RA-FLS

We asked whether SAA-induced PTX3 synthesis in rheumatoid synoviocytes was regulated by FPRL-1. To answer

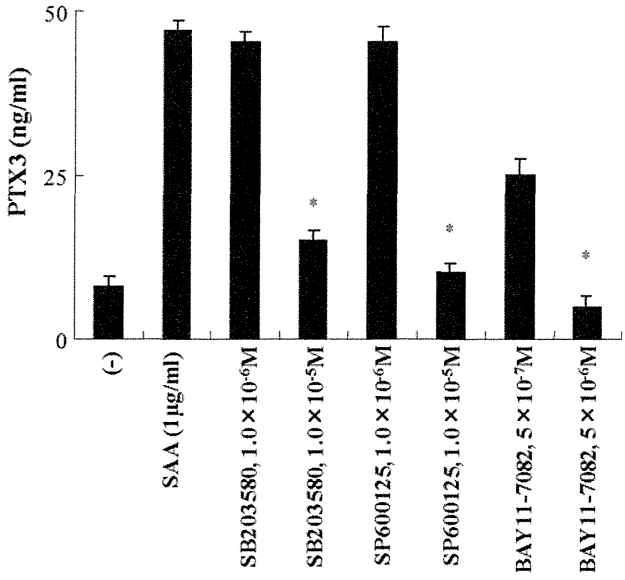

Fig. 5 MAPK or NF-κB inhibition suppressed PTX3 secretion. Rheumatoid synoviocytes were incubated with vehicle (DMSO, media) SB203580 (p38 inhibitor), SP600125 (JNK inhibitor), and BAY11-7082 (NF-κB inhibitor) for 1 h. Cells were then stimulated with 1 μg/mL of SAA for 24 h, after which the medium was collected and the PTX3 content was measured by ELISA. The data are representative of three independent experiments performed using different rheumatoid synoviocytes, and are expressed as the mean ± SEM of results obtained in triplicate. $*p < 0.001$ compared to SAA-treated rheumatoid synoviocytes

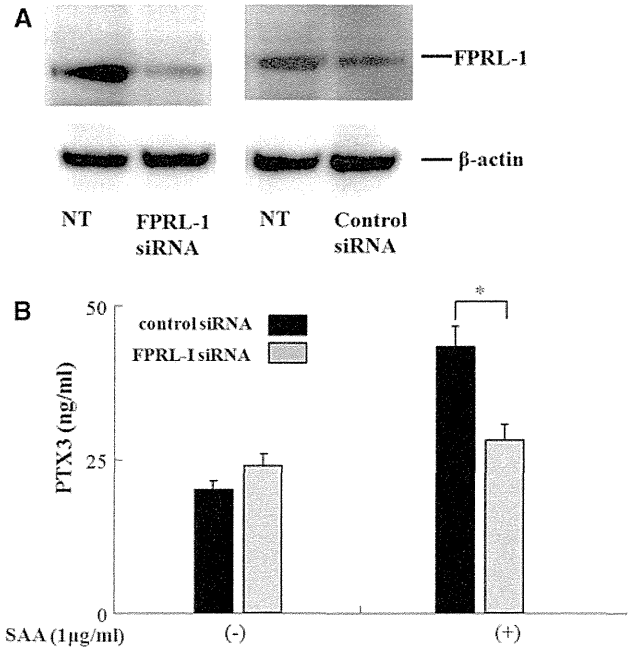

Fig. 6 Effects of FPRL-1 suppression on SAA-induced PTX3 synthesis in rheumatoid synoviocytes. **a** Rheumatoid synoviocytes were transfected with FPRL-1 or control scrambled small interfering RNA (siRNA). Proteins were extracted 24 h after transfection, and western blot was performed using anti-FPRL-1 or anti-β-actin antibodies. The data are representative of two independent experiments performed using different rheumatoid synoviocytes. **b** Twenty-four hours after siRNA transfection, rheumatoid synoviocytes were treated with SAA (1 μg/mL) for another 24 h, after which the medium was collected and the PTX3 content was measured by ELISA. The data are representative of three independent experiments performed using different rheumatoid synoviocytes, and are expressed as the mean ± SEM of results obtained in triplicate. $*p < 0.001$ between FPRL-1 siRNA-treated synoviocytes and control siRNA-treated synoviocytes

this question, we suppressed FPRL-1 expression. Rheumatoid synoviocytes were nucleofected with 100 nmol of control or FPRL-1 siRNA. After 24 h, cells were stimulated with SAA for 24 h. Immunoblotting of cell lysate confirmed a specific decrease in FPRL-1 expression (Fig. 6a). The decreased FPRL-1 expression resulted in a significant reduction in PTX3 secretion from SAA-stimulated rheumatoid synoviocytes (Fig. 6b).

PTX3 expression in OA synoviocytes

Finally, to examine whether SAA-mediated PTX3 induction was limited to rheumatoid synoviocytes, we investigated the effects of SAA on synoviocytes from osteoarthritis (OA) patients. As shown in Fig. 6, SAA significantly induced PTX3 synthesis from OA synoviocytes. However, the ability to induce PTX3 in OA synoviocytes was less than that in RA synoviocytes (Fig. 7).

Discussion

Inflammatory cytokines such as IL-β and TNF-α, as well as microbial components, trigger local expression of PTX3 in macrophages and endothelial cells [5]. In the present study, we evaluated the PTX3 secretion in rheumatoid synoviocytes. We found that cultured rheumatoid synoviocytes synthesized PTX3 after stimulation with SAA, an acute-phase reactant. SAA markedly induced PTX3 expression in rheumatoid synoviocytes at physiological concentrations, and its induction capacity was comparable to that of high concentrations of IL-1β or TNF-α. Elevated levels of PTX3 have been reported in synovial fluids from RA patients [11]. Our findings suggest that, in addition to IL-1β or TNF-α, SAA, which is localized within rheumatoid synovial fluids, also contributes to the elevated expression of PTX3 in rheumatoid synovium.

PTX3 is produced in an IL-6-independent manner [21]. However, our findings suggest that PTX3 could be induced by SAA, in which IL-6 likely contributes to its synthesis [22]. PTX3 is an activator of innate immunity and a modulator of adoptive immunity [3]. For example, PTX3, like the short pentraxin CRP, binds to C1q, the first component of the classical pathway of complement activation [23]. It is tempting to speculate that SAA-induced PTX3

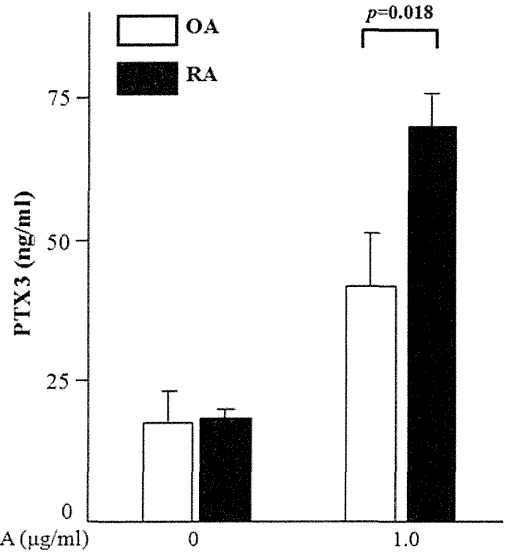

Fig. 7 SAA stimulates PTX3 synthesis in OA synoviocytes. Synoviocytes isolated from three patients with osteoarthritis (OA) or RA patients were stimulated with SAA (1 μg/mL) for 24 h. PTX3 in the conditioned media was determined by ELISA. The data are expressed as the mean ± SD of the results obtained from three independent experiments using three different synoviocytes isolated from three patients with OA or RA. $*p = 0.014$ between SAA (1 μg/mL)-treated OA synoviocytes and RA synoviocytes

may amplify complement-mediated mechanisms that are responsible for inflammation and tissue damage in RA. In addition to the interaction with the classical complement component, PTX3 is a pattern recognition receptor involved in the recognition of and response to microbial elements and damaged tissues [24]. Moreover, evidence suggests that PTX3 acts as a sensor of inflammatory reactions and may contribute to the decoding system, which discriminates between infections (nonself) and apoptotic responses (self) in antigen presentation [25]. Considering these functions of PTX3 in innate immunity and inflammation, SAA-triggered PTX3 may participate in the activation of inflammatory cells and tissue injury in the rheumatoid synovium. This raises the possibility that SAA-induced, local production of PTX3 in rheumatoid synovium contributes to the synovitis and subsequent cartilage destruction observed in RA patients.

MAPKs are known to participate in the signal transduction cascades that control cellular responses to cytokines and stress [26]. We previously demonstrated that signaling events induced by SAA include the activation of MAPKs and NF-κB [20]. In this study, we showed that pharmacological inhibition of both NF-κB and MAPKs suppressed the SAA-induced PTX3 induction. The promoter region of the PTX3 gene has a number of potential binding sites for transcription factors, such as NF-IL-6, NF-κB, and AP-I [27]. Among these transcription factors, NF-κB is essential for the induction of PTX3 mRNA by IL-1 or TNF-α [28]. In addition to this NF-κB-dependent PTX3 expression, JNK-dependent PTX3 expression was reported to occur in different cell types, suggesting the complex regulation of PTX3 expression by different stimuli [21]. Our results suggest that the NF-κB pathway and to some degree the MAPK pathway are involved in SAA-mediated PTX3 induction.

The importance of SAA in various physiological and pathological processes has enhanced the importance of the cell surface receptor that mediates the proinflammatory effects of SAA. SAA has been demonstrated to be a chemoattracting ligand for FPRL-1, a transmembrane G-protein-coupled receptor [14]. We demonstrated that SAA-induced expression of PTX3 was suppressed in FPRL-1-downregulated rheumatoid synoviocytes, suggesting that FPRL-1 mediates SAA-induced PTX3 synthesis. However, it remains unclear as to whether another receptor could be involved in the SAA-induced expression of PTX3 [29], since FPRL-1 knockdown did not completely eradicate the SAA-induced expression of PTX3.

Tissue damage elicits an inflammatory response, which stimulates the rapid synthesis of acute-phase molecules [7]. The systemic inflammatory response induces the expression of different acute-phase reactants, including the pentraxin family [30]. Short pentraxins and SAA are produced in the liver. [1]. In contrast to the short pentraxins, PTX3 is produced at the sites of inflammation [3]. Liver-derived SAA and tissue-derived long pentraxin (PTX3) are thought to be produced independently in response to microbial sensing and cytokines [4].

In conclusion, SAA has been viewed as an acute-phase reactant and an inflammatory biomarker, similar to CRP. In this study, we demonstrated that SAA induces another proinflammatory molecule, PTX3, in rheumatoid synoviocytes. Our data highlight a novel network between SAA and PTX3 in the rheumatoid inflammatory microenvironment, leading to an integrated system that contributes to the fine-tuning of inflammation.

Acknowledgments This work was supported by a Grant-in-Aid for Scientific Research from the Japan Society for the Promotion of Science.

Conflict of interest None.

References

1. Mantovani A, Garlanda C, Doni A, Bottazzi B. Pentraxins in innate immunity: from C-reactive protein to the long pentraxin PTX3. J Clin Immunol. 2008;28:1–13.
2. Bottazzi B, Vouret-Craviari V, Bastone A, De Gioia L, Matteucci C, Peri G, et al. Multimer formation and ligand recognition by the long pentraxin PTX3. Similarities and differences with the short

pentraxins C-reactive protein and serum amyloid P component. J Biol Chem. 1997;272:32817–23.
3. Bottazzi B, Garlanda C, Cotena A, Moalli F, Jaillon S, Deban L, et al. The long pentraxin PTX3 as a prototypic humoral pattern recognition receptor: interplay with cellular innate immunity. Immunol Rev. 2009;227:9–18.
4. Garlanda C, Bottazzi B, Bastone A, Mantovani A. Pentraxins at the crossroads between innate immunity, inflammation, matrix deposition, and female fertility. Annu Rev Immunol. 2005;23: 337–66.
5. Alles VV, Bottazzi B, Peri G, Golay J, Introna M, Mantovani A. Inducible expression of PTX3, a new member of the pentraxin family, in human mononuclear phagocytes. Blood. 1994;84: 3483–93.
6. Deban L, Bottazzi B, Garlanda C, de la Torre YM, Mantovani A. Pentraxins: multifunctional proteins at the interface of innate immunity and inflammation. BioFactors. 2009;35:138–45.
7. Manfredi AA, Rovere-Querini P, Bottazzi B, Garlanda C, Mantovani A. Pentraxins, humoral innate immunity and tissue injury. Curr Opin Immunol. 2008;20:538–44.
8. Muller B, Peri G, Doni A, Torri V, Landmann R, Bottazzi B, et al. Circulating levels of the long pentraxin PTX3 correlate with severity of infection in critically ill patients. Crit Care Med. 2001;29:1404–7.
9. Peri G, Introna M, Corradi D, Iacuitti G, Signorini S, Avanzini F, et al. PTX3, a prototypical long pentraxin, is an early indicator of acute myocardial infarction in humans. Circulation. 2000;102: 636–41.
10. Fazzini F, Peri G, Doni A, Dell'Antonio G, Dal Cin E, Bozzolo E, et al. PTX3 in small-vessel vasculitides: an independent indicator of disease activity produced at sites of inflammation. Arthritis Rheum. 2001;44:2841–50.
11. Luchetti MM, Piccinini G, Mantovani A, Peri G, Matteucci C, Pomponio G, et al. Expression and production of the long pentraxin PTX3 in rheumatoid arthritis (RA). Clin Exp Immunol. 2000;119:196–202.
12. Uhlar CM, Whitehead AS. Serum amyloid A, the major vertebrate acute-phase reactant. Eur J Biochem. 1999;265:501–23.
13. Urieli-Shoval S, Linke RP, Matzner Y. Expression and function of serum amyloid A, a major acute-phase protein, in normal and disease states. Curr Opin Hematol. 2000;7:64–9.
14. He R, Sang H, Ye RD. Serum amyloid A induces IL-8 secretion through a G protein-coupled receptor, FPRL1/LXA4R. Blood. 2003;101:1572–81.
15. Badolato R, Wang JM, Murphy WJ, Lloyd AR, Michiel DF, Bausserman LL, et al. Serum amyloid A is a chemoattractant: induction of migration, adhesion, and tissue infiltration of monocytes and polymorphonuclear leukocytes. J Exp Med. 1994;180:203–9.
16. Furlaneto CJ, Campa A. A novel function of serum amyloid A: a potent stimulus for the release of tumor necrosis factor-alpha, interleukin-1beta, and interleukin-8 by human blood neutrophil. Biochem Biophys Res Commun. 2000;268:405–8.
17. Kumon Y, Loose LD, Birbara CA, Sipe JD. Rheumatoid arthritis exhibits reduced acute phase and enhanced constitutive serum amyloid A protein in synovial fluid relative to serum. A comparison with C-reactive protein. J Rheumatol. 1997;24:14–9.
18. Steiner G, Tohidast-Akrad M, Witzmann G, Vesely M, Studnicka-Benke A, Gal A, et al. Cytokine production by synovial T cells in rheumatoid arthritis. Rheumatology. 1999;38:202–13.
19. Jahangiri A. High-density lipoprotein and the acute phase response. Curr Opin Endocrinol Diabetes Obes. 2010;17:156–60.
20. Migita K, Koga T, Torigoshi T, Maeda Y, Miyashita T, Izumi Y, et al. Serum amyloid A protein stimulates CCL20 production in rheumatoid synoviocytes. Rheumatology. 2009;48:741–7.
21. Han B, Mura M, Andrade CF, Okutani D, Lodyga M, dos Santos CC, et al. TNFalpha-induced long pentraxin PTX3 expression in human lung epithelial cells via JNK. J Immunol. 2005;175: 8303–11.
22. Jensen LE, Whitehead AS. Regulation of serum amyloid A protein expression during the acute-phase response. Biochem J. 1998;334:489–503.
23. Ortega-Hernandez OD, Bassi N, Shoenfeld Y, Anaya JM. The long pentraxin 3 and its role in autoimmunity. Semin Arthritis Rheum. 2009;39:38–54.
24. Agrawal A, Singh PP, Bottazzi B, Garlanda C, Mantovani A. Pattern recognition by pentraxins. Adv Exp Med Biol. 2009; 653:98–116.
25. McGreal EP. Structural basis of pattern recognition by innate immune molecules. Adv Exp Med Biol. 2009;653:139–61.
26. Kaminska B. MAPK signalling pathways as molecular targets for anti-inflammatory therapy—from molecular mechanisms to therapeutic benefits. Biochim Biophys Acta. 2005;1754:253–62.
27. Altmeyer A, Klampfer L, Goodman AR, Vilcek J. Promoter structure and transcriptional activation of the murine TSG-14 gene encoding a tumor necrosis factor/interleukin-1-inducible pentraxin protein. J Biol Chem. 1995;270:25584–90.
28. Basile A, Sica A, d'Aniello E, Breviario F, Garrido G, Castellano M, et al. Characterization of the promoter for the human long pentraxin PTX3. Role of NF-kappaB in tumor necrosis factor-alpha and interleukin-1beta regulation. J Biol Chem. 1997;272: 8172–8.
29. Cheng N, He R, Tian J, Ye PP, Ye RD. Cutting edge: TLR2 is a functional receptor for acute-phase serum amyloid A. J Immunol. 2008;181:22–6.
30. Jensen LE, Hiney MP, Shields DC, Uhlar CM, Lindsay AJ, Whitehead AS. Acute phase proteins in salmonids: evolutionary analyses and acute phase response. J Immunol. 1997;158:384–92.

The Contribution of *SAA1* Polymorphisms to Familial Mediterranean Fever Susceptibility in the Japanese Population

Kiyoshi Migita[1]*, Kazunaga Agematsu[2], Junya Masumoto[3], Hiroaki Ida[4], Seiyo Honda[4], Yuka Jiuchi[1], Yasumori Izumi[1], Yumi Maeda[1], Ritei Uehara[5], Yoshikazu Nakamura[5], Tomohiro Koga[6], Atsushi Kawakami[6], Munetoshi Nakashima[7], Yuichiro Fujieda[8], Fumiaki Nonaka[9], Katsumi Eguchi[9], Hiroshi Furukawa[10], Tadashi Nakamura[11], Minoru Nakamura[1], Michio Yasunami[12]

1 Clinical Research Center, Department of General Internal Medicine and NHO Nagasaki Medical Center, Kubara, Omura, Japan, **2** Department of Infection and Host Defense Graduate School of Medicine, Shinshu University, Asahi, Matsumoto, Japan, **3** Department of Pathogenomics, Ehime University Graduate School of Medicine, Toone City, Ehime, Japan, **4** Department of Rheumatology, Kurume University School of Medicine, Kurume, Japan, **5** Department of Public Health, Jichi Medical University, Tochigi, Japan, **6** First Department of Internal Medicine, Nagasaki University School of Medicine, Sakamoto, Nagasaki, Japan, **7** Department of Rheumatology, Red Cross Nagasaki Atomic bomb Hospital, Mori, Nagasaki, Japan, **8** Department of Medicine II, Hokkaido University Graduate School of Medicine, Sapporo, Japan, **9** Department of Rheumatology, Sasebo City General Hospital, Hirase, Sasebo, Japan, **10** Department of Rheumatology, NHO Sagamihara Hospital, Sakuradai, Sagamihara, Japan, **11** Department of Rheumatology, NTT WEST JAPAN Kyushu Hospital, Shinyashiki, Kumamoto, Japan, **12** Center for International Collaborative Research (CICORN) and Institute of Tropical Medicine, Nagasaki University, Nagasaki, Japan

Abstract

Background/Aims: Familial Mediterranean Fever (FMF) has traditionally been considered to be an autosomal-recessive disease, however, it has been observed that substantial numbers of patients with FMF possess only 1 demonstrable *MEFV* mutation. The clinical profile of familial Mediterranean fever (FMF) may be influenced by *MEFV* allelic heterogeneity and other genetic and/or environmental factors.

Methodology/Principal Findings: In view of the inflammatory nature of FMF, we investigated whether serum amyloid A (SAA) and interleukin-1 beta (IL-1β) gene polymorphisms may affect the susceptibility of Japanese patients with FMF. The genotypes of the -13C/T SNP in the 5′-flanking region of the *SAA1* gene and the two SNPs within exon 3 of *SAA1* (2995C/T and 3010C/T polymorphisms) were determined in 83 Japanese patients with FMF and 200 healthy controls. The same samples were genotyped for IL-1β-511 (C/T) and IL-1 receptor antagonist (IL-1Ra) variable number of tandem repeat (VNTR) polymorphisms. There were no significant differences between FMF patients and healthy subjects in the genotypic distribution of *IL-1β -511* (C/T), *IL-1Ra* VNTR and *SAA2* polymorphisms. The frequencies of *SAA1.1* allele were significantly lower (21.7% versus 34.0%), and inversely the frequencies of *SAA1.3* allele were higher (48.8% versus 37.5%) in FMF patients compared with healthy subjects. The frequency of -13T alleles, associated with the *SAA1.3* allele in the Japanese population, was significantly higher (56.0% versus 41.0%, $p = 0.001$) in FMF patients compared with healthy subjects.

Conclusions/Significance: Our data indicate that *SAA1* gene polymorphisms, consisting of -13T/C SNP in the 5′-flanking region and SNPs within exon 3 (2995C/T and 3010C/T polymorphisms) of *SAA1* gene, are associated with susceptibility to FMF in the Japanese population.

Citation: Migita K, Agematsu K, Masumoto J, Ida H, Honda S, et al. (2013) The Contribution of *SAA1* Polymorphisms to Familial Mediterranean Fever Susceptibility in the Japanese Population. PLoS ONE 8(2): e55227. doi:10.1371/journal.pone.0055227

Editor: Matthaios Speletas, University of Thessaly, Greece

Received May 30, 2012; **Accepted** December 20, 2012; **Published** February 20, 2013

Funding: This work was supported by a Grant-in-Aid for Research on intractable diseases from Ministry of Health, Labour and Welfare of Japan, "Study group of national-wide survey for Familial Mediterranean fever in Japan". The funders had no role in study design, data collection and analysis, decision to publish, or preparation of the manuscript.

Competing Interests: The authors have declared that no competing interests exist.

* E-mail: migita@nmc.hosp.go.jp

Introduction

FMF is an inherited autoinflammatory disease characterized by recurrent self-limited fever, and serositis [1]. These episodes of inflammation are mainly mediated by a massive influx of neutrophils into serous cavities and are accompanied by an elevation of acute phase reactants [2]. The disease is associated with mutations in the *MEFV* gene that encodes pyrin, and is transmitted in an autosomal-recessive manner [3]. Therefore, heterozygotes are expected to be carriers or lack the clinical phenotype of FMF. However, mutations in the second *MEFV* allele have not been observed in 20–30% of patients with typical FMF [4]. Recent studies suggest that subjects with a single *MEFV* mutation may cross a threshold for the development of an FMF phenotype if they also express a combination of gene polymorphisms that favor increased inflammation [5]. These polymor-

phisms are thought to belong to genes of the interleukin-1β/innate immune system pathways [5]. The IL-1 family of cytokines is critical to the host's response to infection, and induction of innate immunity and acute phase inflammation [6]. The overproduction of IL-1β is responsible for a variety of autoinflammatory syndromes including FMF [7]. IL-1β requires cleavage via caspase-1 for proper secretion, which is facilitated by inflammasome activation [8]. The NOD-like receptor family, pryin domain containing 3 (NLRP3) inflammasome has emerged as a critical cytosolic sensor for a number of endogenous mediators, including amyloid protein [9].

Recent studies have shown that serum amyloid A (SAA) induced the expression of pro-IL-1β and activated the NLRP3 inflammasome in a cathepsin B and $P2X_7$-dependent manner resulting in secretion of mature IL-1β [10]. SAA is an acute-phase protein, which increases in the serum during inflammation and is susceptible to proteolytic cleavage to amyloid A (AA) protein, the major fibrillar protein in secondary amyloidosis [11]. An allelic variant of *SAA1.3*, was found to be associated with AA amyloidosis in Japanese rheumatoid arthritis (RA) patients [12]. In view of the recent genetic studies in FMF, other modifying genetic factors may contribute to the susceptibility or clinical expression of FMF in addition to *MEFV* mutations. Therefore, we attempted to determine the effect of gene polymorphisms on the susceptibility to FMF in the Japanese population.

Materials and Methods

Patients

In early 2007, a laboratory network collecting the genetic diagnosis of periodic fever was established at the Japan Autoinflammation Association (JAA), and *MEFV* gene analysis was carried out at the Clinical Research Center of National Hospital Organization (NHO) Nagasaki Medical Center. Up to October 2012, 481 consecutive unrelated patients with periodic fever were referred and underwent molecular diagnosis at the NHO Nagasaki Medical Center. All patient, who were originating from Japan, (East Japan n = 36, West Japan n = 47) were asked to complete a questionnaire that included demographics (sex, age of onset), family history (consanguinity of parents, family history of recurrent fever), and the presence of recurrent febrile attacks typical of FMF, including peritonitis, pleuritis, arthritis, and transient inflammatory responses. The genetic analysis of *MEFV* gene was approved by the Ethics Committee of Nagasaki Medical Center, and written informed consent was obtained from each individual. On the basis of Tel-Hashomer criteria [13], we divided the FMF patients in two groups: Group 1, typical FMF exhibiting the presence of 1 or more major criteria independent to the presence of minor criteria; Group 2, incomplete FMF exhibiting the absence of major criteria and 2 or more minor criteria. It is important to stress that response to colchicine was confirmed in almost all patients. As controls, 200 healthy Japanese individuals without pre-existing medical diseases (90 men and 110 women 14 to 64 years, with a mean age of 38.6±13.9 years) from East Japan (n = 86) and West Japan (n = 114) were enrolled in the study after obtaining informed consent.

MEFV gene Mutation analysis

All patients were undergone genetic analysis of *MEFV* gene exons 1, 2, 3 and 10 by direct sequencing. 2 milliliters of blood samples were collected from all subjects. Genomic DNA was extracted from whole blood by means of the Promega Wizard® Genomic DNA Purification Kit (Promega, USA). Mutation analysis was performed by genomic sequencing as described previously [14].

Genotyping

***SAA1* gene.** The genotype of the SAA1 -13C/T in the 5-region of exon 1 (rs11024595) was determined by the polymerase chain reaction–restriction fragment length polymorphism (PCR–RFLP) method [15]. The primers used for the PCR reaction were 5′-ACATCT TGTTCCCTC AGGTTG-3′ (sense) and 5′-GCTGTAGCTGAGCTGCGG-3′ (antisense).

The 229-bp PCR products were digested with restriction enzyme AciI (BioLabs, Beverly, MA, USA) and electrophoresed on a 12.5% polyacrylamide gel [15].

The *SAA1.1, 1.3*, and *1.5* alleles, corresponding to the T-C, C-T, and C-C haplotypes of the C2995T (rs1136743) and C3010T (rs1136747) polymorphisms were also determined by the PCR-RFLP [15]. The primers used for the PCR reaction were 5′-GCC AATTACATCGGCCTCAG-3′ (sense) and 5′-TGGCCA AA-GAATCTCTGG AT-3′ (antisense).

The 518-bp PCR products were digested with restriction enzyme BclI (Promega, San Luis Obispo, CA, USA) and BanI (Promega) and electrophoresed on a 2.5% agarose gel [15].

The genotype of the *SAA2* (rs2468844) was determined by the polymerase chain reaction–restriction fragment length polymorphism (PCR–RFLP) method. The primers used for the PCR reaction were 5′-AGAGAATATCCAGAGACTCACAGGC-3′ (sense) and 5′-CAGGCCAGCAGGTCGGAAGT-3′(antisense). The 115 bp PCR products were digested with the restriction enzyme Nco I. The digested products were separated by 3% agarose gels by ethidium bromide staining [15].

IL-1Ra. For the IL-1RA VNTR polymorphism, the region including variable numbers of identical 86-bp tandem repeats was amplified by PCR using the following primers: 5′-CTCAGC-CAACACTCCTAT-3′ (sense) and 5′-TCCTGGTCTGCAGG-TAA-3′ (antisense). PCR products of 240(allele 2, two repeats), 325 (allele 3, three repeats), 410 (allele 4, four repeats), and 500 bp (allele 5, five repeats) were distinguished by agarose gel electrophoresis [16].

IL-1B-511. A fragment containing the *AvaI* polymorphic site at promoter region -511 of the IL-1B gene was amplified by PCR. PCR was carried out with primers, forward primer 5′-GCCTGAACCCTGCATACCGT-3′ (sense). 5′-GCCAA-TAGCCCTTGTCT-3′ (antisense). Fragments were separated by electrophoresis on 3% agarose with ethidium bromide staining using appropriate commercially available size markers for comparison. The C allele was designated if two bands of 92 and 63 bp were obtained, and the T allele was designated if a signal band of the undigested 155 bp was obtained. Genotypes were designated as follows: C/C, two bands of 92 and 63 bp: C/T, three bands of 155, 92, and 63 bp; and T/T, a single band of 155 bp [16].

Statistical Analysis

Results are expressed as mean±SD. Statistical analysis was performed with SPSS18 for windows (SPSS Statistics, Illinois). The statistical significance of differences between groups was calculated by either the chi-square test for categorical data and Mann-Whitney's U-test for quantitative data. Deviation from Hardy-Weinberg equilibrium was assessed using the SNPAlyze software ver. 7.0 (Dynacom, Yokohama, Japan). A p value of <0.05 was considered significant.

Table 1. *MEFV* genotypes, gender, and the presence of amyloidosis in 83 Japanese patients with FMF.

MEFV genotypes	n(%)	Typical	(Male/Female)	Incomplete	(Male/Female)	Amyloidosis	*p* value
M694I/M694I	4(4.8)	4	(1/3)			1	
M694I/normal	4(4.8)	4	(4/0)				
M694I/E148Q	13(15.7)	13	(10/3)				
M694I/P751L	1(1.2)	1	(0/1)				
M694I/E148Q/E148Q	1(1.2)	1	(0/1)				
M694I/E148Q/L110P	5(6.0)	5	(3/2)			2	
P369S/R408Q	4(4.8)			4	(1/3)		
E148Q/P369S/R408Q	3(3.6)			3	(0/3)		
E148Q/E148Q/P369S/R408Q	4(4.8)	2	(2/0)	2	(0/2)		
E148Q/R202Q/P369S/R408Q	1(1.2)			1	(1/0)	1	
E148Q/G304R/P369S/R408Q	1(1.2)			1	(0/1)		
E148Q/E148Q/P369S/P369S/R408Q/R408Q	1(1.2)			1	(0/1)		
E148Q/normal	12(14.5)	6	(3/3)	6	(1/5)		
R202Q/normal	2(2.4)	1	(1/0)	1	(0/1)		
G304R/normal	1(1.2)			1	(1/0)		
E148Q/E148Q	1(1.2)	1	(0/1)				
E148Q/L110P	6(7.2)	1	(0/1)	5	(1/4)		
E148Q/R202Q	1(1.2)	1	(0/1)				
E148Q/E148Q/L110P	3(3.6)	1	(1/0)	2	(2/0)		
E148Q/L110P/R202Q	2(2.4)			2	(0/2)		
E84K/normal	8(9.6)	5	(3/2)	3	(1/2)		
E84K/E148Q	1(1.2)			1	(0/1)		
E84K/G304R	1(1.2)			1	(0/1)		
Normal	3(3.6)			3	(1/2)		
Gender (Male/Fmale)			(28/18)		(9/28)		$P<0.0001$
Age (years)			36.2±18.2		39.9±19.6		$p=0.419$
Total			46		37		

Data are expressed as number (percentage). ± ; standard deviation. *p* values were calculated with chis-square test for qualitative data and Mann-Whitney test for quantitative data.

doi:10.1371/journal.pone.0055227.t001

Results

Demographic data and MEFV genotypes

We diagnosed 83 subjects, all of Japanese origins, as FMF. Among these patients, 44 were diagnosed as typical FMF and 37 were diagnosed as incomplete FMF. The demographic data of the newly-diagnosed FMF patients are summarized in Table 1. The overall male: female ration in patients with FMF was 0.8 (37:46). In incomplete FMF patients, the more affected sex is female in contrast to typical FMF (Table 1). The mean age ± SD at diagnosis was 37.9±18.8 years. Age at diagnosis of patients with typical FMF was similar to those with incomplete FMF (36.2±18.2 and 39.9±19.6 years, respectively; $p=0.419$; Table 1). By mutation analysis, the *MEFV* gene mutation could not be identified in 3 of 83 patients (3.6%). The distribution of the *MEFV* genotype was heterogenous. The most frequent genotype was M694I/E148Q, followed by E148Q/normal and E84K/normal. AA amyloidosis was histologically confirmed in 4 patients with FMF, whose genotypes were M694I/M694I *SAA1.5/15*, M694I/E148Q/L110P *SAA1.1/1.1*, M694I/E148Q/L110P *SAA1.3/1.5* and E148Q/R202Q/P369S/R408Q *SAA1.3/1.5*.

IL-1β and *IL-1Ra* gene polymorphism

The genotype frequencies of IL-1β-511 (C/T), and IL-1Ra VNTR polymorphisms in FMF patients and healthy subjects are summarized in Table 2. There were no significant difference in the frequencies of these polymorphisms between FMF patients and healthy subjects.

Association between *SAA2* gene polymorphism and FMF

There was no significant difference in the frequencies of the *SAA2* genotype between FMF patients and healthy subjects (Table 2).

Association between *SAA1* gene polymorphisms and FMF

A segment of the genomic *SAA1* gene with polymorphic sites was subjected to PCR/restriction fragment length polymorphism (PCR-RFLP) analysis. Table 3 shows the frequencies of individuals with various genotypes and alleles at the *SAA1* locus in either FMF patients (n = 83) or Japanese healthy subjects (n = 200). The allele frequency of *SAA1.1* was significantly lower in FMF patients compared with healthy subjects (21.7% versus 34.0%). Conversely,

Table 2. Frequencies of the genotypes at the *IL-1β* -511, *IL-1Ra* and *SAA2* loci in patients with FMF and healthy subjects.

	FMF patients	Healthy subjects	*p* value
	n = 83(%)	n = 200(%)	
Genotype at *IL-1β* -511 locus			
C/C	27(32.5)	59(29.5)	$\chi^2 = 0.934$ $p = 0.627$
C/T	43(51.8)	100(50.0)	
T/T	13(15.7)	41(20.5)	
Genotype at *IL-1Ra* locus			
1/1	73(88.0)	167(83.5)	$\chi^2 = 2.451$ $p = 0.857$
1/2	5(6.0)	20(10.0)	
1/3	0	1(0.5)	
1/4	4(4.8)	7(3.5)	
2/2	0	2(1.0)	
2/4	1(1.2)	3(1.5)	
Genotype at *SAA2* locus			
A/A	62(74.7)	163(81.5)	$\chi^2 = 2.338$ $p = 0.276$
A/G	19(22.9)	35(17.5)	
G/G	2(2.4)	2(1.0)	

IL-1β; Interleukin-*1β* .*IL-1Ra*; Interleukin-1 receptor antagonist .*SAA2*; Serum amyloid A2. Chi-square test was used to examine differences of genotype and allele frequencies between FMF patients and healthy subjects.
doi:10.1371/journal.pone.0055227.t002

the allele frequency of *SAA1.3* was higher in FMF patients compared with healthy subjects (48.8% versus 37.5%).

The -13C/T polymorphism, in the 5′-flanking region of the *SAA1* gene is associated with the *SAA1.3* allele and susceptibility to amyloidosis in Japanese RA patients [17]. We analyzed the frequency of -13C/T polymorphisms in FMF patients and Japanese healthy subjects. Allele frequencies of -13C/T were different among these two groups (Table 4), and -13T allele was significantly increased in FMF patients compared with healthy subjects (56.0% versus 41.0%, $p = 0.001$). These data suggest that the -13T allele is associated with susceptibility to FMF in the Japanese population. Allele frequencies of -13 C/T polymorphisms were also analyzed in typical or incomplete FMF patients. There was no significant difference in the frequencies -13T allele between typical and incomplete FMF patients (Table 5). Among 83 patients with FMF, 30 patients had 0 to 1 *MEFV* mutation (no mutation 3; heterozygous 27) and 53 patients at least 2 mutations (homozygous or compound heterozygous). There was no significant difference in *SAA1* gene polymorphisms between FMF patients with different numbers of *MEFV* mutations (Table 6).

Hardy-Weinberg equilibrium test

Finally, Hardy-Weinberg equilibrium was estimated by chi-square test with Yates' correction. There was no significant difference between observed and experienced frequencies of each genotype (*SAA1* -13C/T, *SAA2*, *IL-1β-511*) in the both FMF patients (Table 7) and healthy subjects (Table 7). These results indicated that these populations had a relatively stable genetic background and were stable for genetic statistical analysis.

Table 3. Frequencies of the genotypes and alleles at the *SAA1* locus of Japanese patients with FMF and healthy subjects.

	FMF patients	Healthy subjects	*p* value
	n = 83(%)	n = 200(%)	
Genotype at *SAA1* locus			
1.1/1.1	4(4.8)	24(12.0)	$\chi2 = 12.553$ $p = 0.028$
1.1/1.3	22(25.6)	49(24.5)	
1.1/1.5	6(7.2)	39(19.5)	
1.3/1.3	15(18.1)	27(13.5)	
1.3/1.5	29(34.9)	47(23.5)	
1.5/1.5	7(8.4)	14(7.0)	
Allele at *SAA1* locus			
1.1	36(21.7)	136(34.0)	$\chi2 = 9.563$ $p = 0.008$
1.3	81(48.8)	150(37.5)	
1.5	49(29.5)	114(28.5)	

SAA1; Serum amyloid A1. Chi-square test was used to examine differences of genotype and allele frequencies between FMF patients and healthy subjects.
doi:10.1371/journal.pone.0055227.t003

Discussion

FMF is considered to be an autosomal recessive disease [18]. The gene causing FMF is *MEFV*, which encodes pyrin, expressed in the cytoplasm of myeloid cells [2]. Pyrin is postulated to act as a negative regulator of IL-1-mediated inflammation [19]. However, approximately 30% of FMF patients exhibit a single *MEFV* mutation, despite sequencing of the entire *MEFV* genomic region and other autoinflammatory genes [20]. More recently it was demonstrated that pyrin truncation in mice did not show an overt phenotype of FMF, however, pyrin-deficient and FMF-associated B30.2 mutations "knock in" mice showed severe spontaneous inflammatory phenotype, suggesting that FMF may be caused by a gain of function by disease-associated missense changes in pyrin

Table 4. Frequencies of the genotypes and alleles at -13C/T *SAA1* locus of Japanese patients with FMF and healthy subjects.

	FMF patients	Healthy subjects	*p* value
	n = 83(%)	n = 200(%)	
Genotypes at -13C/T *SAA1*			
C/C	13(15.7)	67(33.5)	$\chi^2 = 11.538$ $p = 0.003$
C/T	47(56.6)	102(51.0)	
T/T	23(27.7)	31(15.5)	
Alleles at -13C/T *SAA1*			
T	93(56.0)	164(41.0)	$\chi^2 = 10.682$ $p = 0.001$
C	73(44.0)	236(59.0)	

SAA1; Serum amyloid A1. Chi-square test was used to examine differences of genotype and allele frequencies between FMF patients and healthy subjects.
doi:10.1371/journal.pone.0055227.t004